Effects of soiling and weathering on the albedo of building envelope materials: lessons learned from natural exposure in two European cities and tuning of a laboratory simulation practice

Riccardo Paolini[1,2,3*], Giancarlo Terraneo[4], Chiara Ferrari[5], Mohamad Sleiman[3,6], Alberto Muscio[5], Pierangelo Metrangolo[4], Tiziana Poli[1], Hugo Destaillats[3], Michele Zinzi[7], Ronnen Levinson[3]

Accepted for publication in

Solar Energy Materials and Solar Cells

https://doi.org/10.1016/j.solmat.2019.110264

©2019. This manuscript version is made available under the CC-BY-NC-ND 4.0 license

http://creativecommons.org/licenses/by-nc-nd/4.0/

Highlights

- We selected sixteen roofing and four wall finish products
- We naturally aged them for four years in Rome and Milan and exposed them in the lab
- The mean absolute albedo difference (natural – lab) of roofing products is 0.027
- ASTM D7897 can be adapted to mimic weathering and soiling out of the U.S.A.
- We identified possible improvements to natural aging and lab exposure practices

Graphical Abstract

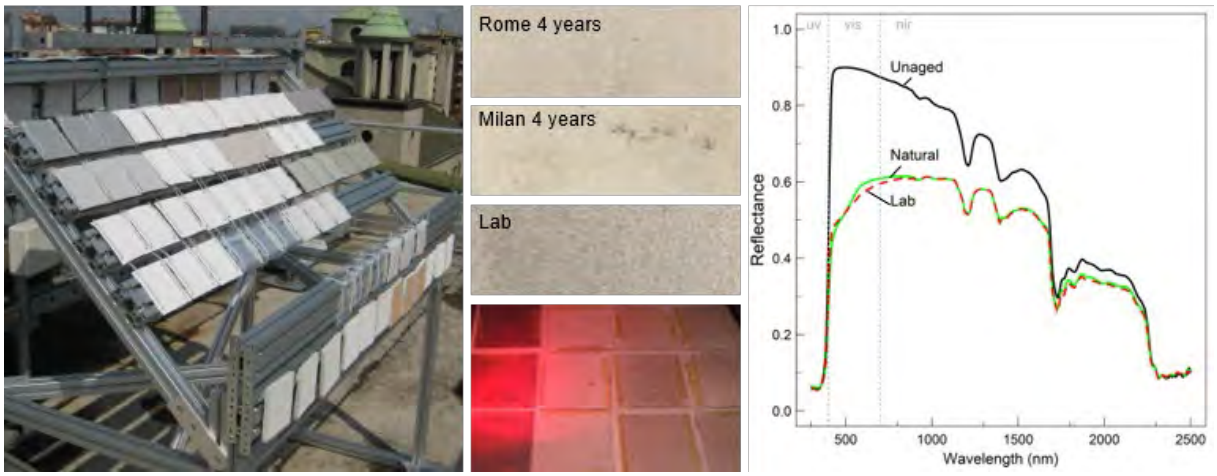

[1] Politecnico di Milano, Department of Architecture, Built environment and Construction engineering, Milano, Italy
[2] The University of New South Wales, Faculty of Built Environment, UNSW Sydney, Australia
[3] Heat Island Group, Energy Technologies Area, Lawrence Berkeley National Laboratory, Berkeley, CA, USA
[4] Politecnico di Milano, Department of Chemistry, Materials and Chemical Engineering "Giulio Natta", Milano, Italy
[5] Universitá degli Studi di Modena e Reggio Emilia, Dipartimento di Ingegneria Enzo Ferrari, Modena, Italy
[6] Université Clermont Auvergne, CNRS, SIGMA Clermont, Institut de Chimie de Clermont-Ferrand, F-63000 Clermont–Ferrand, France
[7] ENEA – UTEE-ERT Italian National Agency for New Technologies, Energy and Sustainable Economic Development, Roma, Italy

* Corresponding author. Emails: r.paolini@unsw.edu.au, RPaolini@LBL.gov – Current address: Faculty of Built Environment, Red Centre West Wing, UNSW Sydney, NSW 2052, Australia

Disclaimer

This document was prepared as an account of work sponsored by the Italian Revenue Agency and the Italian Ministry of Economic Development, with the initial stages of the laboratory exposure adaptation supported also by the United States Department of Energy. Part of the data analysis was conducted while at the University of New South Wales, Australia, with Riccardo Paolini's position sponsored by the fund Anita Lawrence Chair in High Performance Architecture at the Faculty of Built Environment. While this document is believed to contain correct information, neither the Italian Government, the United States Government, nor any agency thereof, nor the Research Institutions to which the authors are affiliated, nor any of their employees, make any warranty, express or implied, or assumes any legal responsibility for the accuracy, completeness, or usefulness of any information, apparatus, product, or process disclosed, or represents that its use would not infringe privately owned rights. Reference herein to any specific commercial product process, or service by its trade name, trademark, manufacturer, or otherwise, does not necessarily constitute or imply its endorsement, recommendation, or favouring by the Italian or the United States Government or any agency thereof, or the Research Institutions to which the authors are affiliated. Further, the dataset does not make any reference to commercial products and commercial technologies and the data cannot be used neither to promote nor denigrate any product or company.

Abstract

Chemical and physical stress, weathering, organic and inorganic matter deposition, and microbial growth over time, or "aging", affect the optical-radiative performance of building envelope materials. Natural exposure helps to quantify these effects, but it usually requires several years. Further, the contribution of the different degradation agents cannot be isolated, and results from different campaigns cannot be easily compared because of the variability in the boundary conditions producing aging. Here we present an adaptation of the protocol implemented by ASTM as D7897-18 "Standard Practice for Laboratory Soiling and Weathering of Roofing Materials to Simulate Effects of Natural Exposure on Solar Reflectance and Thermal Emittance". The aim is to reproduce in the laboratory the changes in albedo (solar reflectance) and thermal emittance experienced by building envelope materials in European urban areas rather than in the United States. We tuned the spraying duration and weathering cycles, and we compared the UV-vis-NIR reflectances of naturally-aged specimens (48 months in Rome and Milan) of roofing and wall finish materials to those exposed to laboratory weathering and soiling. Excluding those materials that show early physical-chemical degradation, the mean absolute deviation between natural and laboratory exposure of roofing products is equal to 0.027 in albedo. This is a lower value than the differences between two natural exposure campaigns at the same site. We clearly defined the limits of application of the protocol, providing an appraisal of the repeatability of natural aging. Moreover, we identified possible improvements in the methodology to conduct both natural and laboratory exposure.

Keywords: weathering; soiling; aging; natural exposure; laboratory exposure; reflectance.

1. Introduction

Global and local climate change can be mitigated by the large-scale retrofit of built environments with surfaces having high solar reflectance (ρ), or "albedo", and high thermal emittance (ε), known as cool materials [1]. Cool roofs can also offset CO2, and a reduce the building cooling needs [2,3], which are increasing due to global climate change, growing urbanization, and a deepened market penetration of air conditioning [4]. Per unit surface area, cool walls savings can equal or exceed cool roof savings as often energy codes prescribe less wall than roof insulation [5], and at pedestrian height can produce peak air temperature reductions of ~ 0.08 °C per 0.10 increase in wall albedo [6]. Moreover, the risk of thermal shocks decreases with increasing wall albedo [7].

For highly reflective materials, the greatest challenge is not to provide enhanced performance, but to offer it during their whole service life in use in the built environment, which is the broad concept of durability (i.e., "the ability of a product to maintain its required performance over a given or long time, under the influence of foreseeable action" [8,9]). In fact, weathering, chemical and physical stress, organic and inorganic matter deposition, and microbial growth over time, or "aging", affect the optical and radiative response of building envelope materials [10,11], reducing the cooling savings offered by cool materials [7,12]. The effects of aging on the albedo of building materials are consistently documented by outdoor exposure campaigns performed in the US [13,14], Europe [7,12,15], South America [16,17], Japan [18,19], and China [20,21]. The main ingredients of soiling are approximately the same in all urban contexts [15], with a dominant role of black carbon [14]. Black carbon, or soot, has an absorption coefficient decreasing with the wavelength, with weak spectral dependence of the motor vehicle aerosols [22]. In addition to roofing membranes [12], albedo losses also affect clay tiles [17], and wall renders [7]. Even the self-cleaning effect of photocatalytic materials is impaired by soiling, because a thick layer of depositions reduces the number of high-energy photons reaching the surface, weakening the photoactivation [23–25]. The de-pollution effect is also affected by soiling [26], while weathering contributes to the recovery of the self-cleaning performance [27]. Physical degradation may also induce an apparent self-cleaning behavior when pristine surface is exposed after the detachment of aged portions [28]. Then, biofouling produces an additional significant reflectance drop [14,29,30]. Biological colonization starts only upon a layer of organic or inorganic matter is deposited on the surface of the exposed material, becoming a growing medium favorable to the development of biofilms [31,32]. Biofouling does not develop on any surface, but only on those that offer favorable surface temperature, moisture content, pH and other conditions, for a sufficient time, exceeding the minimum time for germination, depending on the type of spores [33].

While in the United States aged values for albedo and thermal emittance are provided by the Cool Roofing Rating Council (CRRC) and the US EPA [13,34], only small datasets from experimental programs are available elsewhere [7,12,16–21]. Natural exposure is time-consuming as obtaining reliable results at times may require several years [10], and short-term results can be affected by the year and season of exposure [12].

A laboratory method has been developed to mimic the effects of environmental exposure on the solar reflectance and thermal emittance of roofing products exposed in the United States [14]. This method has been approved by ASTM as D7897-18 "Standard Practice for Laboratory Soiling and Weathering of Roofing Materials to Simulate Effects of Natural Exposure on Solar Reflectance and Thermal Emittance" [35]. ASTM D 7897-18 was validated

with a natural exposure campaign with a separate set of samples from the set used to train the protocol, but at the same sites where the training exposure took place. Therefore, to expand the validity of the protocol, there is the need for external validation, with natural exposure at other sites from the development context. Moreover, the existing method was not designed to mimic weathering and soiling out of the United States; then its portability or adaptability to different climate and pollution contexts needs to be assessed. Additional gaps in the existing knowledge about weathering and soiling of building envelope materials include the appraisal of the variability in the results achieved with aging campaigns started at different times and the minimum necessary duration of the exposure.

Here we present an extension of the application of a method developed for roofing products exposed in the United States to polluted European urban areas (and, in general, to urban areas), and to wall finish coats[1]. We focus on the limits of application of the laboratory exposure protocol, identifying which degradation features and dynamics cannot be reproduced reliably. Finally, we discuss possible improvements to natural and laboratory exposure practices, also by using samples with different durability.

2. Methods

2.1. Materials

We selected roofing and wall finishing materials from the European market including 14 roofing membranes; two clay roofing tiles; and four wall finishes (Table 1). All the selected membranes are for both low and steep roofing applications. These products were chosen since they are made of different materials, offering different spectral reflectance, photoactive and non-photoactive features, smooth or rough surface, and different propensity to aging. The purpose of this selection is to provide an initial set of diverse properties to test a laboratory protocol, investigating a broad spectrum of aging mechanisms and phenomena both with natural and laboratory exposures. In natural aging programs, the exposure of one or two materials of known durability to act as reference or control samples is commonly recommended [38,39]. The manufacturer, after internal UV testing, declared membrane M05 as unsuited for exterior applications. Thus, we used M05 as a benchmark, to test if soiling is influenced by physical and chemical aging or is just a surface phenomenon. Membranes M11 and M12 were not exposed to laboratory weathering and soiling. Images of all the membranes are available with early results of the exposure [12], while the characterization and self-cleaning performance of M10 and W03 (together with their control samples M08 and W04) are also documented in previous work [25,28]. W01 and W02 finish coats have a siloxane-based binder and display a rough surface [7], while W03 and W04 are cement-based [28].

[1] With finish coats here we refer to the top coating, providing decorative finish and protection against weathering, applied over the reinforced base coats used for exterior insulation wall systems [36,37].

Table 1. Selected building envelope products and initial solar reflectance and thermal emittance.

Code	Description	Initial solar reflectance	Initial thermal emittance
M01	Grey flexible polyolefin (matte and with anti-slip surface)	0.26	0.94
M02	Grey flexible polyolefin with white factory-applied elastomeric coating (glossy)	0.81	0.90
M03	White flexible polyolefin (matte and with anti-slip surface)	0.76	0.94
M04	White thermoplastic polyolefin (glossy)	0.82	0.93
M05	Grey PVC membrane.	0.46	0.93
M06	White PVC membrane (matte)	0.85	0.92
M07	Cool beige thermoplastic polyolefin (matte)	0.59	0.93
M08	Modified-bitumen with extra white field-applied coating	0.81	0.92
M09	Modified-bitumen with white field-applied coating	0.73	0.92
M10	Modified-bitumen with white TiO_2 photoactive field applied coating	0.76	0.91
M11	Modified-bitumen with white field-applied coating type B (glossy)	0.72	0.91
M12	Modified-bitumen with cool colored field-applied coating	0.39	0.91
M13	Photoactive asphalt roll (modified-bitumen with granules)	0.28	0.93
M14	Standard asphalt roll (modified-bitumen with granules)	0.23	0.94
T01	Red clay tile	0.47	0.88
T02	White paint on clay tile	0.73	0.89
W01	Beige wall finish coat (rough)	0.45	0.94
W02	White wall finish coat (rough)	0.73	0.94
W03	White fiber reinforced mortar (photoactive)	0.74	0.94
W04	White fiber reinforced mortar (standard)	0.68	0.94

2.2. Measurement of reflectance and emittance

Following ASTM E903-12 "Standard Test Method for Solar Absorptance, Reflectance, and Transmittance of Materials Using Integrating Spheres" [40], the solar spectral reflectances were measured clean and aged in the center point of each membrane from 300 to 2,500 nm with a resolution of 5 nm. We characterized small specimens of clay roofing tiles (~ 4 cm × 4 cm) at two points per specimen. Then, at the end of the exposure, we sampled the full size tiles obtaining smaller fragments, on which at least ten different scans were carried out. Thus, we calculated the broadband reflectances (e.g., solar reflectance) by averaging the solar spectral reflectance weighted with the air mass one global horizontal (AM1GH) solar spectral irradiance [40,41]. The uncertainty in the measurement of the solar reflectance is of ± 0.02 [40,42]. In this study, we used two PerkinElmer Lambda 950 spectrophotometers, each with a 150 mm Labsphere integrating sphere, one in Milan and one in Rome. To assess the reproducibility, we selected a subset of roofing membranes for which the standard deviation of unaged solar reflectance is less than 0.0035 (i.e., M01, M04, M05, M06, and M07), performing measurements on three unaged samples per material. Thus, we computed that the mean absolute deviation between the solar reflectances measured in Milan and Rome is 0.004, with the

maximum absolute difference between the two instruments equal to 0.008. We performed three measurements per sample on non-overlapping spots on three samples to determine the standard deviation.

We performed five thermal emittance measurements per sample, on unaged and aged specimens at the end of the exposure. We used a TIR 100-2 emissometer by Inglas, in the range between 2.5 µm and 40 µm (with declared accuracy of ± 0.01 for samples with high emittance), measuring a spot of 5 mm on samples greater than 7 cm in diameter. This device implements the measurement method detailed in EN 15976: 2011 "Flexible sheets for waterproofing - Determination of emissivity" [43]. The measurement uncertainty of thermal emittance has been determined as equal to ± 0.02 [42,44]. The unaged values for the clay tiles given in Table 1 have been measured with Devices & Services Portable Emissometer model RD1 AE1, in accordance with ASTM C1371-15 "Standard Test Method for Determination of Emittance of Materials Near Room Temperature Using Portable Emissometers" [45]. This was necessary since we could not obtain flat specimens of the tiles large enough for the TIR 100-2. We selected the radiometric method of EN 15976 because it offers a lower standard deviation than the calorimetric method of ASTM C1371-15 [42].

2.3. Natural exposure

In April 2012 the selected products were exposed on rooftops in Rome (41.933° N, 12.465° E, 35 m above mean sea level) and Milan (45.480° N, Long: 9.229° E, 123 m above mean sea level). For each product, three replicates of size 10 cm × 10 cm were exposed for each site and exposure condition. The specimens were fastened to metal frames (Figure 1), with the lowest row of samples 80 cm above the roof [12]. At 3, 6, 12, 18, 24, 36, and 48 months of natural aging, the same samples were retrieved, measured in the lab, staying unexposed for about one week each time, and returned to the racks. The samples were protected with non-sticky backing foil to prevent undesired contamination or cleaning during handling. Clay roofing tiles were exposed in full size with 30% slope, with replicates facing north and south, extending their aging to 60 months to reach a stable value. Small specimens of 4 cm × 4 cm were also exposed with the same slope. Hereafter, we refer to aging time as the period in months after the start of the exposure and indicated as T followed by the number of months (e.g., T3 for the first three months of aging). The roofing membranes were exposed with 1.5% slope facing south (equal to ~ 0.86°, for simplicity referred to as "horizontal" exposure hereafter) according to application guidelines [46,47]. In Milan, replicate samples were also exposed tilted 45° south. Wall finish materials were vertically exposed in Milan only, facing north and south, unsheltered and sheltered, namely, protected from the rainfall by the top horizontal element of the racks [48,49]. The latter reproduces a small overhang (protruding by 5 cm from the plane of the samples), similar to a window sill or a roof gutter, for instance. In addition, a second horizontal exposure campaign started in Milan in April 2013, with a subset of eight roofing membranes, to assess the inter-campaign variability (i.e., same site and materials, but a different start of the exposure). These include the roofing membranes from M02 to M11, as coded in Table 1.

Both urban areas are polluted (Table S1 and Figure S1, supplementary material). Milan has a continental temperate climate, with cold winters and hot summers, weak wind circulation, and a dry urban climate [50]. Rome, about 30 km far from the coast, has a Mediterranean climate, with mild winters and average wind speed [51]. The conditions in Milan were monitored by a weather station located at the exposure site [52], and by an air quality station

(Città Studi – Pascal) at 250 m [53]. In Rome, the exposure site is located approximately halfway between two air quality stations located within urban parks [54], and weather data are retrieved from an urban station at 5 km [55].

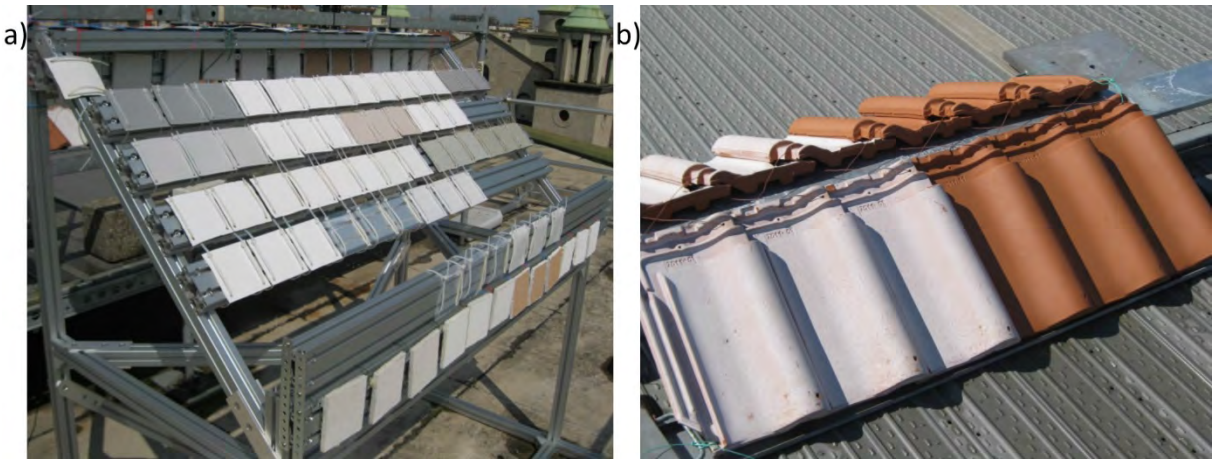

Figure 1. Exposure setup in Milan, Italy. (a) Metal rack. Image shows the low sloped membranes specimens on the plate on top of the rack, which shelters the wall finish specimens, while unsheltered specimens are on the lower beams. All specimens are fastened and spaced in a way to avoid cross-contamination and dripping from the fastening system. (b) Clay tiles exposed facing north and south with a 30% slope.

2.4. Laboratory exposure

ASTM D7897-18 reproduces at low cost and in a short time span (less than one week) the effects of environmental exposure on the solar reflectance and thermal emittance of building envelope materials at three sites in the USA (in Phoenix, Arizona; Miami, Florida; and Medina, Ohio), or on the three-site averages of these properties [14,35]. Only the Ohio site, at the fringes between suburban and rural area close to Cleveland (41.123° N, 81.905° W), is moderately polluted [56]. Instead, the Arizona site is in a xeric shrubland ~20 km from the suburbs of Phoenix (33.898° N, 112.158° W), and the Florida exposure farm is at the boundaries of a suburban area between Miami and the Everglades (25.460° N, 80.501° W) [57]. A consequence of the requirement of a rapid assessment – which is the condition for wide use by the industry – is that only a limited number of aging cycles can be performed. This short exposure produces negligible physical/chemical degradation of materials, while the current practice for roofing membranes, for instance, is to conduct UV aging for 500, 1000, or even 2000 hours [58]. Thus, neither ASTM D7897-18 nor the laboratory exposure of this study are referred to as accelerated aging. The repeatability and reproducibility of the ASTM D 7897-18 protocol were tested in a nine-participant interlaboratory study [59]. The repeatability standard deviation ranged from 0.008 to 0.015, while the reproducibility standard deviation ranged from 0.022 to 0.036.

Here we present an adaptation of ASTM D7897-18 to mimic the exposure in Rome and Milan, tested with data from 48 months of aging. The procedure is composed by three identical weathering cycles (W) as in [14], and by two soiling cycles (S), performed in between (it is thus W1 + S1 + W2 + S2 +W3). Similar to natural aging tests, three specimens were exposed to laboratory weathering and soiling (Figure 2). Each weathering cycle has a duration of 24 hours, plus the transients needed to reach the set-point conditions in the chamber (here a QUV by Q-Lab Corp.; Westlake, OH). Each weathering cycle is composed of two repetitions of two sub-cycles including exposure to ultraviolet light (UVA, peak wavelength at 340 nm) and moisture at high temperatures, as in Cycle 1 of ASTM G154-12 “Standard Practice for

Operating Fluorescent Ultraviolet (UV) Lamp Apparatus for Exposure of Nonmetallic Materials" [60]:

- 8 h of UVA 0.89 W/m^2/nm @ 340 nm, with black panel temperature at 60 °C; and
- 4 h of water condensation with black panel temperature at 50 °C.

The soiling agent consists of an aqueous mixture of dust minerals (0.575 g L^{-1}), black carbon (0.0625 g L^{-1}), humic acid (0.35 g L^{-1}), and salts (0.25 g L^{-1}) [14]. The mixture, once prepared, is agitated, and then put into a vessel pressurized at 97 - 103 kPa (Figure 2a), which is connected to a spraying nozzle vertically positioned about 40 cm over the sample to be soiled.

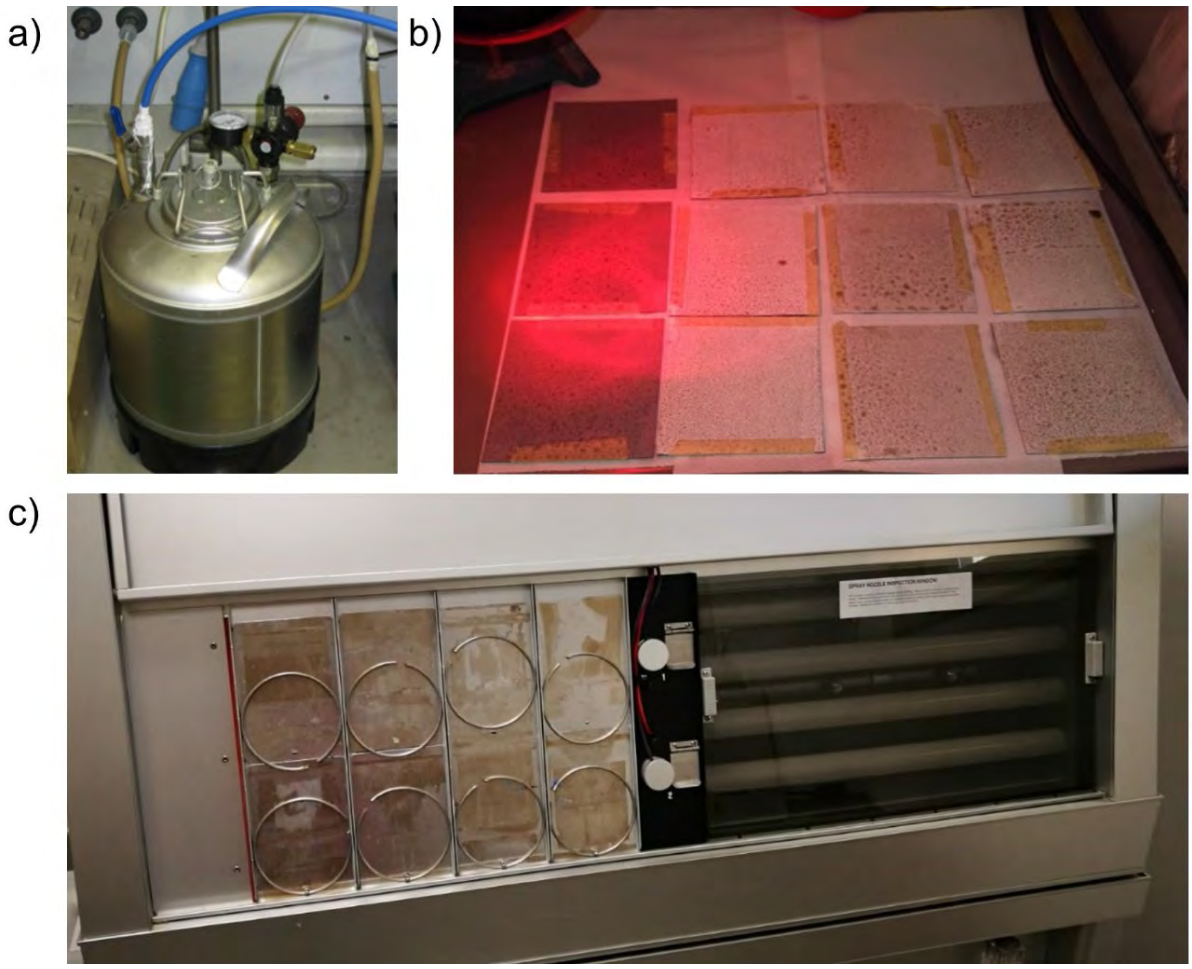

Figure 2. Experimental apparatus for laboratory weathering and soiling. (a) Pressurized vessel to spray the soiling mix; (b) infrared lamp to dry the sprayed samples; and (c) weathering chamber for the exposure to UV and high temperature condensation.

At the beginning and after every fifth coupon soiled, a calibration coupon is soiled and weighed to verify and maintain a consistent spraying time required to achieve the desired wet soiling mass to be sprayed onto the samples. We performed two soiling cycles (instead of one of the original protocol): one after the first and another after the second weathering cycle. In each soiling cycle, 80-90 g m^{-2} of aqueous solution (wet soiling mass) was sprayed onto the roofing material samples. After the first experimental campaigns, to decrease the standard deviation in the depositions, we tried to minimize the impact of the human error on the wet mass deposition, thus reducing the ratio of the reaction time of the operator to the total spraying time. Moreover, high concentrations of the soiling mix may lead to suspended particles forming a precipitate in the tank, reducing the repeatability and increasing the risk of nozzle clogging.

As high pressures lead to short spraying times, we achieved the best results providing the minimum pressure to avoid dripping. Then, we performed each soiling cycle in two steps, of 15 s and 10 s, respectively. Splitting the soiling cycle into two steps also helped to reduce the excessive accumulation of droplets on the surface of the specimen, with undesired runoff. After each soiling step, we dried the samples under an infrared heat lamp (100 W, Figure 2b). We selected a lamp with reduced power compared to the original protocol (250 W) to minimize the risk of degradation of the samples during the drying process. After previous developments of this protocol variant, we also discarded the use of a ventilated oven, because the fan spreads the droplets over the specimen surface. After the first tests, the drying bench was set up adjacent to the hood under which the spraying was performed, to minimize the undesired runoff while handling the specimens.

3. Results and discussion

3.1 Natural exposure

The roofing membranes show significant albedo losses (unaged minus aged) both in Milan and Rome after natural aging. During the four years of the campaign, the minimum albedo is not always achieved at the end of the exposure because of fluctuations due to rain-wash or deterioration of the crust of soiling itself. Considering the minimum measured values, and computing a regression on the measured data, a low sloped cool roof with initial albedo 0.80 is subject to a loss of 0.27 in Milan, and of 0.19 in Rome (Figure 3a). The result of the regression on the measured values at four years, instead, does not significantly differ from the general trend observed at two years (Figure 3b) [12]. The tilted exposure in Milan has shown an intermediate behavior – between the low sloped exposures in Milan and Rome – with maximum albedo losses of 0.21 with initial albedo of 0.80. Materials with initial albedo of 0.20-0.30, instead, after aging were almost showing the initial values.

Most of the membranes reached a stable albedo after 18-24 months of natural aging and in some cases, already after 12 months (Figures S2 and S3, supplementary material). The losses are more pronounced in the visible than in the near infrared range, with a lower dispersion of results in the latter (Figure S4, supplementary material).

After three years, only the albedo of M05 (a grey PVC membrane) is not stable yet due to relevant physical degradation, as expected since it was declared unsuited for unprotected applications by the manufacturer, and selected as a benchmark for this reason. This shows that the physical and chemical degradation of the materials interacts with the soiling process, which is not a merely “cosmetic” deposition of organic or inorganic matter. In Milan, starting in the third year of exposure, we observed biological growth on membranes M07 (a beige polyolefin), M08 and M09 (both white field-applied coatings on modified bitumen).

The solar reflectances of several membranes were higher at 36 months than at 24 months. This is likely due to the climatic anomaly of the summer of 2014 in Northern Italy (i.e., at months 26 and 28 of exposure). Between mid-April and mid-October, it was exceptionally rainy, with 600 mm of rainfall, while usually the yearly precipitation amount is 850 - 900 mm (measured by the weather station at the exposure site). Another aspect that probably contributed to the recovery of reflectance is the detachment of micron-sized portions of paint (chalking). This phenomenon is also observed for cementitious materials [28]. Therefore, we decided to use as naturally aged albedo the minimum measured over the time span of four years (and the five years value for the clay roofing tiles).

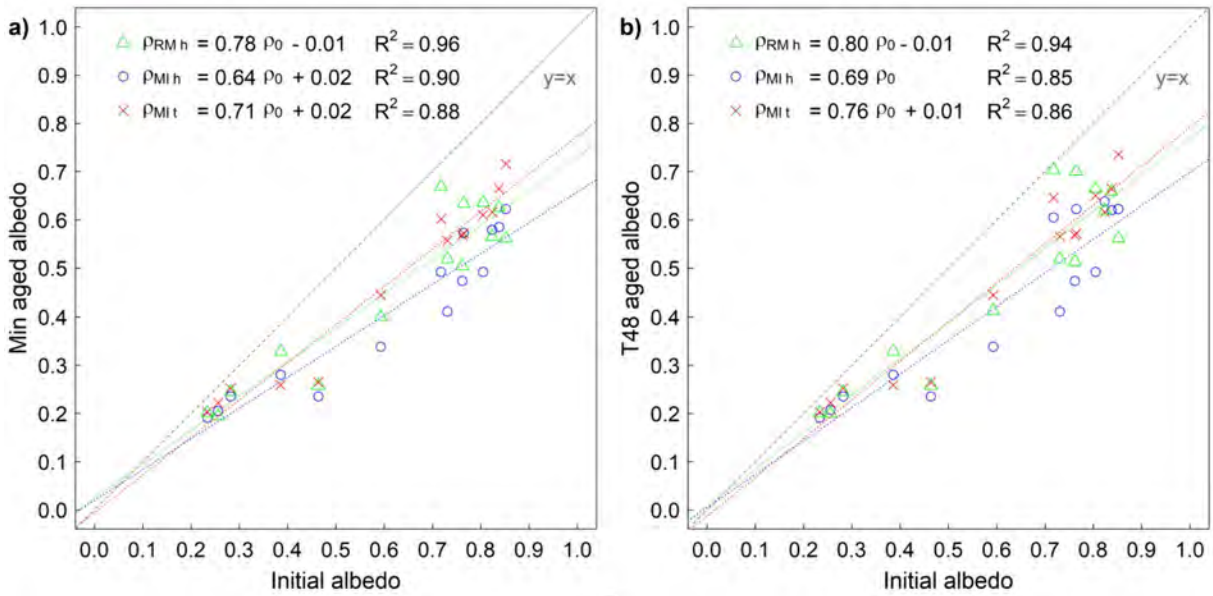

Figure 3. Regressions to initial albedo of (a) minimum albedo measured in the first 48 months and (b) albedo measured at 48 months, shown for horizontal exposure in Rome and Milan and tilted exposure in Milan.

The wall finish coats (W01 - beige and W02 - white) reached a stable trend only after four years, with a 0.20 albedo loss (initial minus final) for the white finish coat exposed in Milan (Figure S3, supplementary material and more details in [7]). The fiber-reinforced mortars (W04) are subject to a less pronounced albedo loss than the finish coats (0.10 for the photoactive and 0.06 for the standard mortars) also because of physical disintegration producing an apparent self-cleaning, especially evident for the standard mortars. The photoactive mortars (W03) are subject to deactivation and loss in self-cleaning performance – as previously observed with a separate two-year campaign at the same site [28] – by approximately 20% already after one year of exposure and stabilizing afterward. After 60 months of exposure, the albedo loss (initial albedo minus aged albedo) for T01 samples (terracotta clay tiles) exposed in Rome and Milan reaches 0.07. T01 samples exposed in Rome and facing north showed the maximum albedo loss (i.e., 0.16), while the minimum was for samples exposed in Rome and facing south (i.e., 0.04). Also in Milan, we measured greater albedo losses for north facing than south facing samples. Albedo losses for white coated clay tiles (T02) range from 0.07 in Milan facing south to 0.19 in Rome facing north. We note that T02 samples exposed in Rome were yellowed by pollination just before T36. As expected from the exposure campaigns conducted in the U.S. [14], since none of the selected materials has a low initial thermal emittance, the changes upon aging are within ± 0.02, namely equal to the measurement uncertainty [42,44].

We used the second exposure campaign to assess the repeatability of natural aging. For some membranes, such as those with an anti-slip surface that provides traction (M03), tilt and year of exposure do not seem to yield to very different results from the horizontal exposure of 2012 (Figure S2, supplementary material). For membranes subject to early physical degradation (M05), the albedo losses do not vary with any exposure condition in Milan but show different intensity in Milan and Rome (Figure S2, supplementary material). However, location and tilt affected the aged albedos of smooth and glossy specimens more than those of rough specimens (Figure S3, supplementary material). This occurs as for these products the influence of rain on the solar reflectance is strongest, especially for the tilted exposure. For the roofing membranes at 36 months of aging, the difference in albedo between the two horizontal exposures in Milan

(2012 minus 2013 exposure) was -0.07 to +0.02 (median -0.02) (Figure 4). The median difference between the two sites (Milan horizontal 2012 minus Rome) is of 0.04 (range between 0.01 and 0.11), with the greatest interquartile range for the difference horizontal and sloped exposures (Milan 2012 horizontal minus Milan tilted).

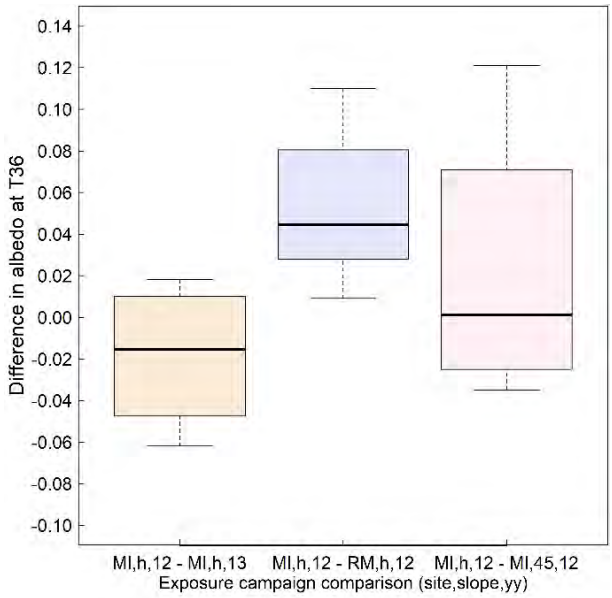

Figure 4. Boxplots of the difference in albedo between the Milan 2012 horizontal and the other exposure campaigns (Milan 2012 minus Milan 2013, Rome 2012, or Milan tilted) of roofing membranes. The x-axis labels indicate the site (MI for Milan and RM for Rome), the slope (h for low sloped and 45° for tilted) and the start year of the exposure (2012 or 2013).

The 2012 Milan titled and 2013 Milan horizontal campaigns show a strong influence of tilt and year of exposure even at the same site, with tilt providing, for the majority of exposed materials, greater dispersion of results than a different exposure site (i.e., Rome 2012 horizontal). However, for rough samples, tilt is less influent than the location on the albedo loss (Figures S2 and S3, supplementary material). Moreover, for some materials such as photoactive ones, the most influent factor between tilt and location changes with time. Therefore, we cannot identify a single predominant factor among tilt, site, and year of exposure.

These results highlight the importance of the selection of the benchmark provided by natural exposure campaigns for the development of laboratory protocols and additionally strengthen the need for control samples when exposing new materials and products, which is already recommended [38,39]. Here we argue that more than one or two control products, displaying different features, shall be used to achieve comparable results gathered with exposure campaigns started at different times or location. In particular, the control samples should offer a variety of characteristics that influence their response to aging, covering at least the range of different features of the new materials to be tested. These features, for instance, include the contact angle or wettability, surface roughness, porosity, and solar reflectance. A robust method to select and use the control samples is the object of future research.

3.2 Laboratory exposure

To test the ability of the laboratory procedure to mimic the effects of weathering and soiling on building envelope materials, we compare the solar reflectance of the replicate specimens exposed in the laboratory to the minimum of the two-site average (Milan 2012 and Rome horizontal) observed within 48 months of exposure (Figure 5a). The laboratory exposure

mimics the natural reflectance loss with a poorer performance compared to the original method (i.e., Lab = 1.08 Nat + 0.01 with R^2 = 0.92 vs Lab = 1.02 Nat - 0.01 with R^2 = 0.96 in [14]).

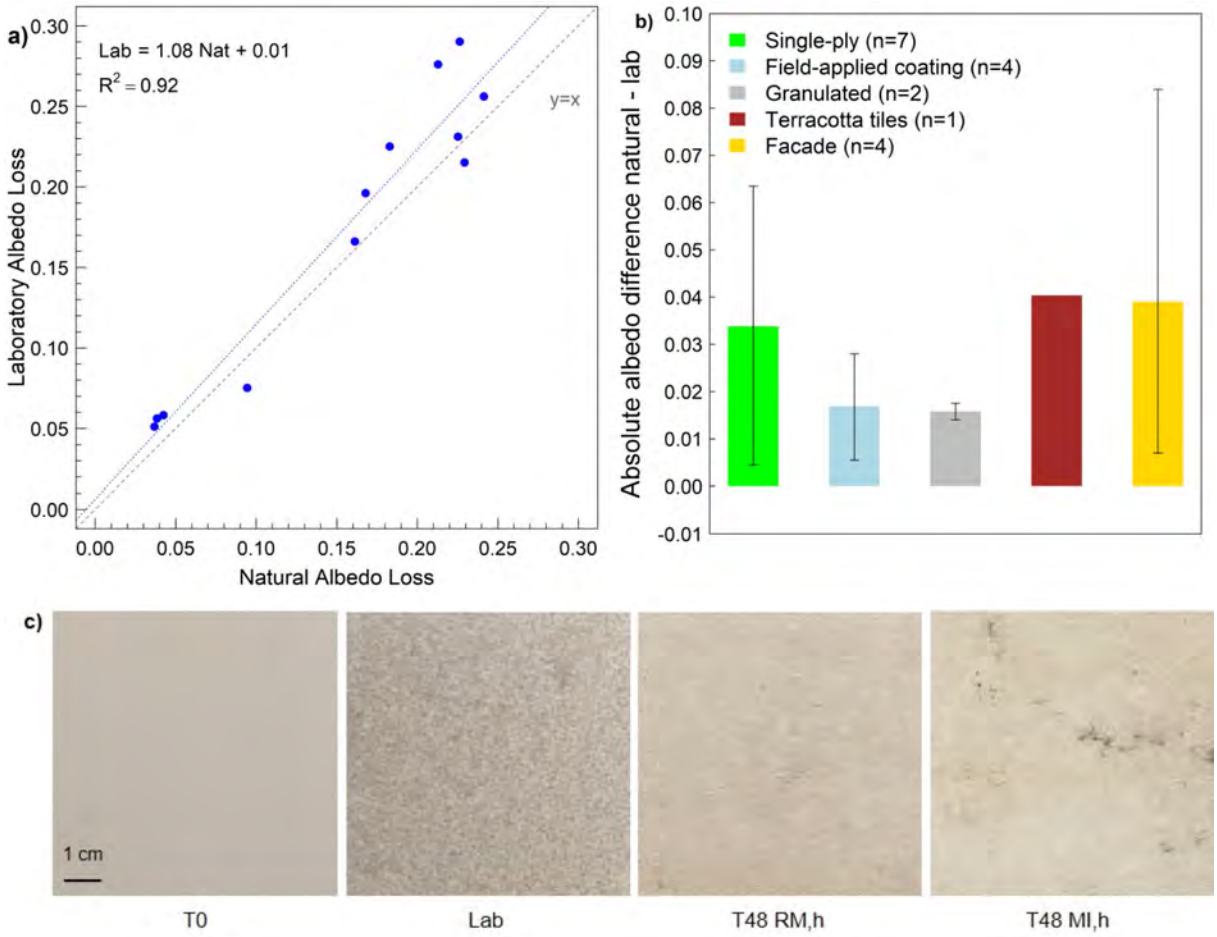

Figure 5. Comparison between laboratory and natural exposure. (a) Regression to natural of laboratory albedo loss for the roofing membranes and (b) absolute albedo difference between natural and lab exposure for all products (the whiskers indicate the maximum and minimum). (c) Images of M03 samples as unaged, after lab exposure, and 48 months of low sloped exposure in Rome and Milan.

This can be in part be expected as we did not include metal roofing products in this study, which typically are almost unaffected by soiling and biological growth, if not at all (Figure 4c of [13]). Most importantly, the wet mass deposited on the surface of the samples is twice what indicated in ASTM D 7897-18 [35], which is necessary to mimic the reflectance loss in European polluted urban areas. In fact, in Rome, the peak concentration of PM2.5 and PM10 is comparable to that of the most polluted among the three CRRC exposure sites, namely Medina, Ohio [56], while in Milan both quantities are approximately twice than in Rome (Table S1 and Figure S1, Supplementary material). We increased the wet mass instead of the concentration of the soiling agents after preliminary tests manifested the risk of clogging the nozzles and dripping, especially at low pressures. Secondly, longer spraying times performed in two stages achieved better uniformity of the deposition and less clustering of the particles on the surface of the sample. This yields the additional advantage of minimizing the changes to the original protocol, therefore simplifying a later standardization of the adapted procedure.

In addition, Milan and Rome are urban sites, while only one of the three U.S. exposure farms (in Ohio) is located in a moderately polluted suburban area, with the other two not exposed to high PM2.5 and PM10 concentrations. The low environmental pollution contributes

to low albedo losses at the CRRC site in Arizona (i.e., 0.08 for roofing products with initial albedo ≥ 0.80), with the average of the albedo losses at the Ohio and Florida sites (i.e., 0.20) closer to the average albedo losses (i.e., 0.23 for roofing membranes with initial albedo of 0.80) in Rome and Milano [13]. Then, the low sloped exposure at the U.S. sites is performed with a tilt angle of 5° [13], which is representative of the slope of metal roofing, but not of flat roofs with single-ply membranes [46,47]. With tilt playing a greater influence on the albedo loss of smooth surfaces than location and year of exposure (Figure 4, and Figures S2 and S3, supplementary material), a part of the greater albedo loss at the Italian than U.S. aging sites can be explained by the different exposure slope.

For the same product categories herein considered, the U.S. three-site average albedo loss equals 0.13 for an initial albedo of 0.80 (Figure S5a, supplementary material), while it is of 0.23 for the considered Italian sites (Figure 3a). In the U.S. the exposure is performed for 36 months, while in this study, we aged the clay tiles for 60 months and all the other materials for 48 months. However, the minimum albedo in Milan and Rome is achieved before 36 months of natural aging for the majority of the roofing membranes (Figures S2 and S3, supplementary material). Hence, the greater albedo loss at the Italian exposure sites and the consequent need of greater wet mass of the soiling mix than for the U.S. is not only the result of the prolonged exposure.

The single-ply membranes and the wall finish materials show the largest absolute difference between natural and laboratory ($\Delta\rho_{NL}$, defined as the absolute value of the natural minus laboratory exposure albedo). While on average $\Delta\rho_{NL}$ is less than 0.04, for the single-ply membranes the maximum $\Delta\rho_{NL}$ is 0.065 (with an average of 0.035) and 0.085 for the wall materials (0.04 on average). Considering only the roofing products, the mean $\Delta\rho_{NL}$ equals 0.027 (Figure 5b). The original protocol showed similar maximum $\Delta\rho_{NL}$, namely equal to 0.06, with the root mean square deviation between natural (three-site average) and laboratory exposure equal to 0.028 [14]. Also in that case, some naturally aged samples presented early degradation and were therefore excluded. In this study, M05 and T02 were excluded from the natural-lab exposure comparison because they presented early degradation. T02 samples were also showing visible signs of biological colonization. However, these differences between natural and laboratory exposure do not exceed the differences due to the campaign, site, or tilt (Figure 4).

A closer scrutiny of the aged solar spectral reflectances characterizes and quantifies what the present protocol cannot reproduce: biological growth (Figure 6), and relevant chemical and physical degradation. Biofouling became visually manifest on some membranes, almost only in Milan, between the third and fourth year of aging, after growing in the deposited organic and inorganic matter [31]. The protocol underpredicts the reflectance loss due to biological growth on the surface (e.g., by 0.04 for the TPO membrane in Figure 6b), still with an acceptable match in many cases. However, this is out of the scope of the current procedure, and the inclusion of a biofouling step in the laboratory exposure is part of further ongoing investigation and development [32]. In fact, excluding the results when biological colonization is visually detectable, we see that the laboratory procedure is capable of mimicking even complex spectral features (Figure 6a). While the original protocol compared with natural aging at the Florida site showed a mismatch mostly concentrated in the visible range (Figure 11c of Ref. [14]), here we observe the maximum reflectance difference (natural minus laboratory) approximately between 600 nm and 1500 nm. This might indicate different types of biological colonization producing different effects.

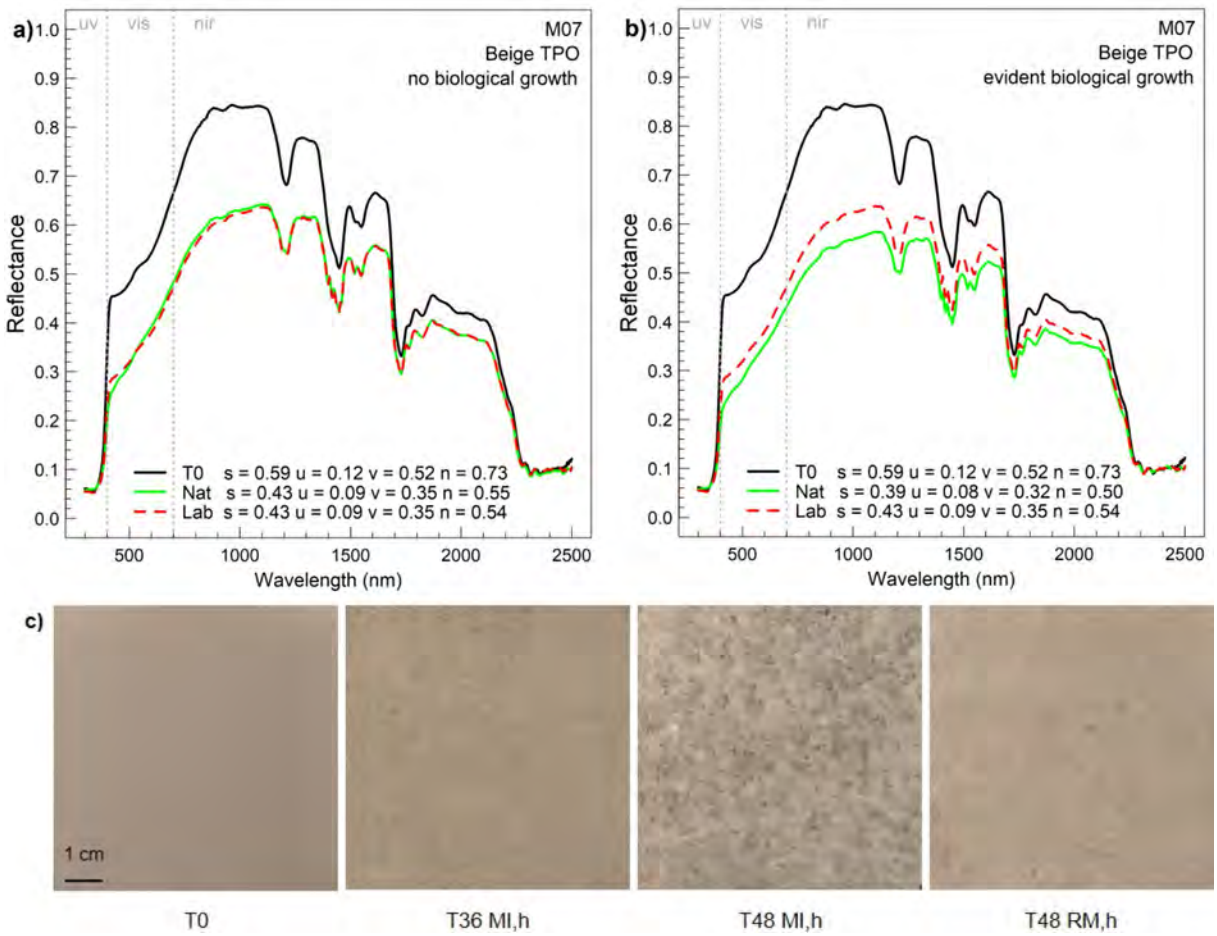

Figure 6. Solar spectral and computed broadband solar (s), UV (u), visible (v), and near infrared (n) reflectance of M07, a beige polyolefin membrane, (a) not showing evident biological growth at 36 months of aging (May 2015) and (b) showing evident biological growth at 48 months aging (May 2016). (c) Images of M07 samples as unaged, after low sloped exposure for 36 and 48 months in Milan, and 48 months in Rome.

The protocol can be applied out of the context of development reproducing aged spectra of a different set of materials simply tuning the amount of deposed wet mass because the aged spectra at different sites are translated along the y-axis, with no significant impact on the spectral signature (Figure 8 of [12]). This can be explained considering that all the soiling agents are present in all contexts, though with a different mix [15].

The reflectance loss of very smooth products is slightly overpredicted (Figure 7a, m02, i.e., a smooth factory-applied coating on a TPO membrane), while the protocol achieves the best performance with products showing a rougher surface (Figure 7b, M03 with anti-slip surface). The original protocol does not claim to assess the effects on solar reflectance and thermal emittance of changes in physical and chemical properties [14], but it was not proven if the soiling can mask the physical degradation or this has a relevant impact on the aged spectra. Here we demonstrate that this aspect cannot be neglected, by considering the extreme case of a grey PVC membrane that was indicated by the manufacturers as unsuited for unprotected applications and included the campaign as a control (Figure 7c). Therefore, a preliminary durability screening is necessary even if assessing the soiling performance only, which is influenced by physical-chemical degradation.

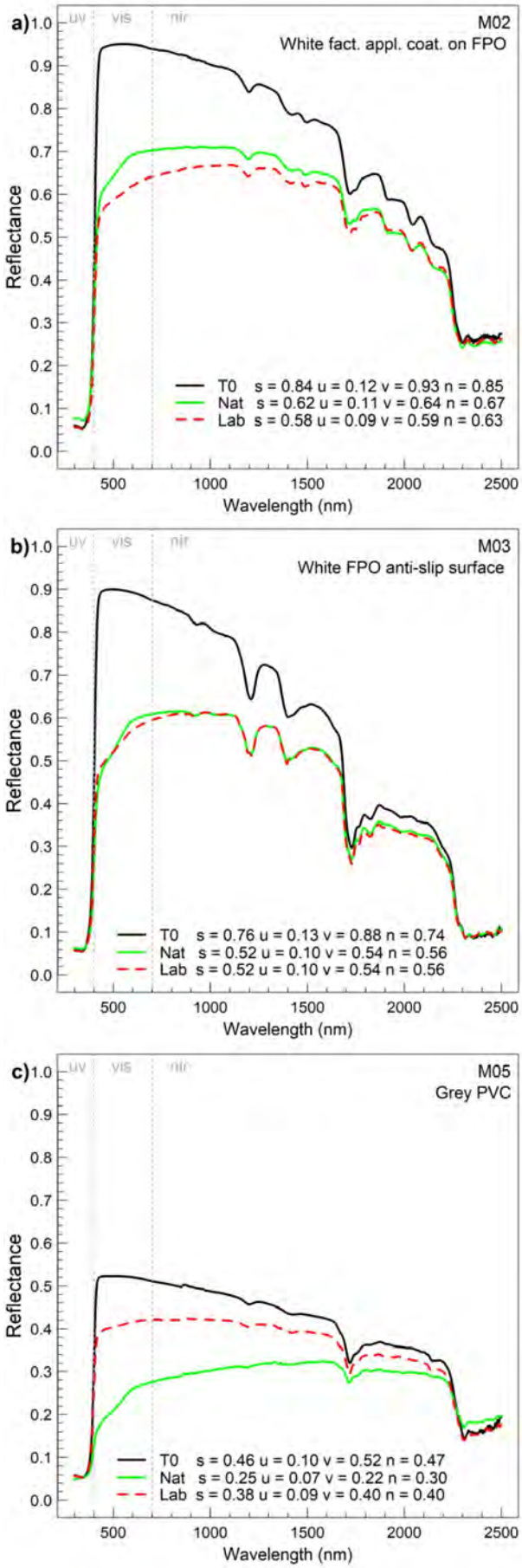

Figure 7. Laboratory vs. natural exposure of roofing membranes. Solar spectral reflectance and computed broadband solar (s), UV (u), visible (v), and near infrared (n) reflectance before (T0) and after natural (Nat) and laboratory exposure (Lab) of: a) white factory applied coating on polyolefin (M02), b) anti-slip white polyolefin (M03), and c) grey PVC unsuited for exterior use (M05), included in the study as a control material.

A good fit between the reflectances of laboratory and naturally aged samples is also observed for wall materials that do not present evidence of relevant physical degradation (Figure 8a,b), which however were exposed in Milan only. Also in this case, we infer that the laboratory exposure overestimation of the reflectance loss by the white standard mortar may be related to the lack of a freeze-thaw phase or other aging cycles that might reproduce the physical degradation (Figure 8c). This happens as delamination, chalking, erosion, or any other similar degradation mechanism produce the detachment of portions of soiled layers, exposing the unsoiled material underneath, with an apparent self-cleaning performance [24,28]. We noticed these dynamics for any material presenting some degree of physical degradation (e.g., some of the field-applied coatings or the coated terracotta tiles).

Furthermore, we verified that reproducing the self-cleaning performance of photoactive materials may result challenging as soiling reduces the amount of UVA radiation reaching the material surface and thus photoactivation [23,28], while weathering may induce a positive effect [27]. Whether these intertwined dynamics can be reliably reproduced by a laboratory procedure shall be clarified by future research. The laboratory procedure slightly overestimates the reflectance loss for the TiO2 containing W03 in the visible range (Figure 8b). Moreover, even a short laboratory UV irradiation can induce the same increase in the last portion of the near infrared observed with natural aging, which signals the production of nitric acid at the surface after photoactivation [25].

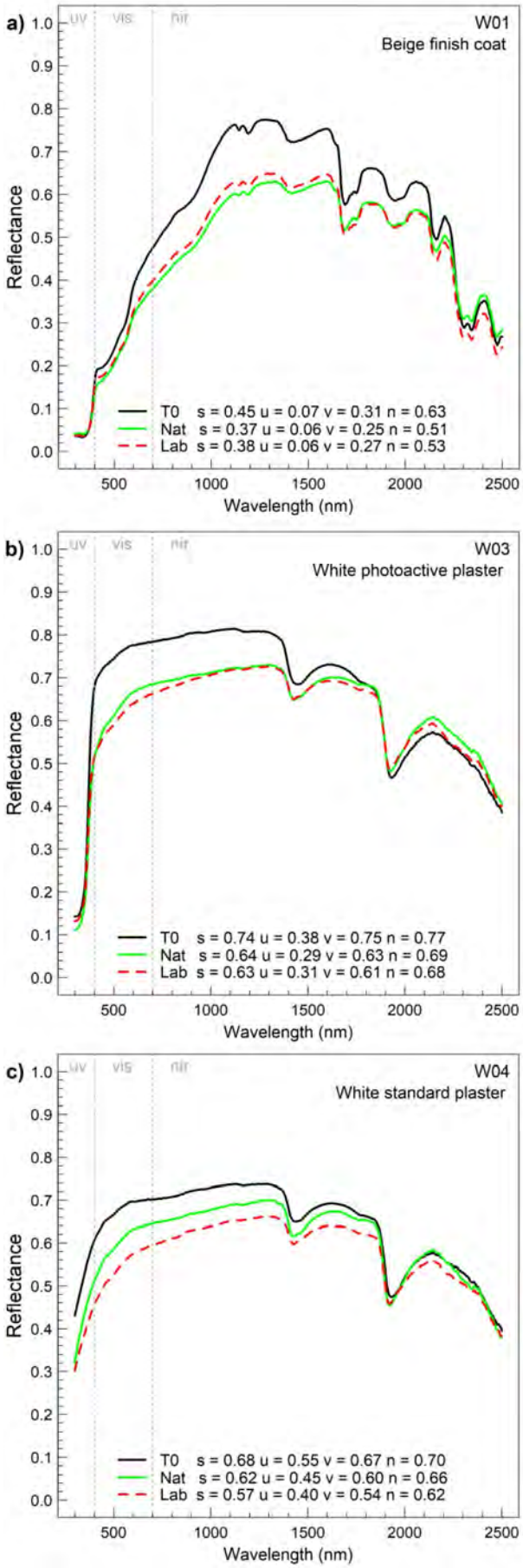

Figure 8. Laboratory vs. natural exposure of wall finish materials (Milano only). Solar spectral reflectance and computed broadband solar (s), UV (u), visible (v), and near infrared (n) reflectance before (T0) and after natural (Nat) and laboratory exposure (Lab) of: (a) a beige finish coat (W01); (b) a white photoactive mortar (W03); and (c) a white standard mortar (W04).

All these differences between laboratory and natural exposure results shall be considered in the context defined by the large inter-site and inter-campaign differences (Figure 4), previously discussed, and by the standard deviation of natural and laboratory exposure (Figure 9). In particular, the inter-campaign differences show that the performance of a laboratory protocol should be compared with multiple campaigns (e.g., three) to account for climatic and air quality variability (Figure 4), instead of a single campaign. The laboratory exposure produces in all the spectral regions a lower standard deviation than low sloped exposure both in Rome and Milan and of the same order of magnitude of the tilted exposure, with the interquartile range within 0.02 and the maximum standard deviations of less than 0.03. The standard deviations of the repeatability and reproducibility of the ASTM D7897-18 protocol, respectively equal to 0.008-0.015 and 0.022-0.036, are less than the maximum standard deviation for low sloped exposure (Figure 9) and less than the difference between exposure campaigns at the same site (Figure 4) [59].

Finally, we do not observe significant changes in the thermal emittance after natural or laboratory exposure (Figure 10), with absolute differences from the initial values that are within the measurement uncertainty [42,44], as expected for non-metallic materials [14]. In this case, we did not measure the emissivity of the aged roofing tiles, as these were destroyed at T60 producing flat fragments too small to be measured with the selected method [43]. However, we do not expect relevant changes in thermal emittance with aging, as for the clay tiles exposed at the CRRC sites (Figure S5b, supplementary material).

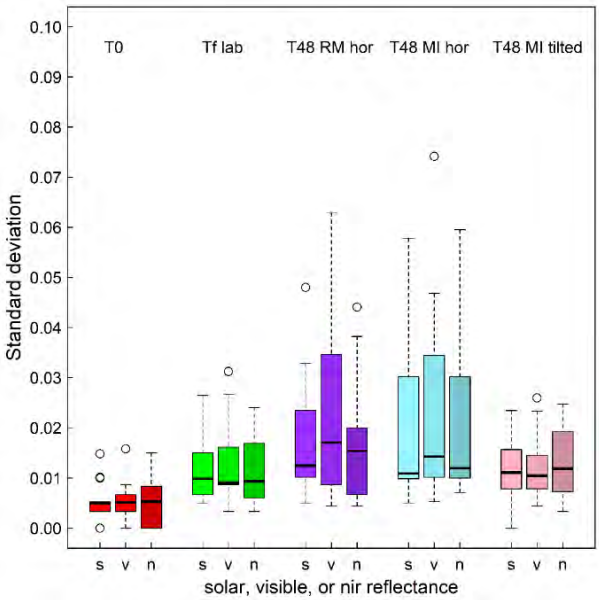

Figure 9. Boxplots of the standard deviations of solar (s), visible (v) and near infrared (n) reflectance of roofing membranes unaged (T0), exposed in the laboratory (Tf lab), and upon four years of environmental low sloped exposure in Rome (T48 MR hor), in Milan (T48 MI hor) and tilted in Milan (T48 MI tilted).

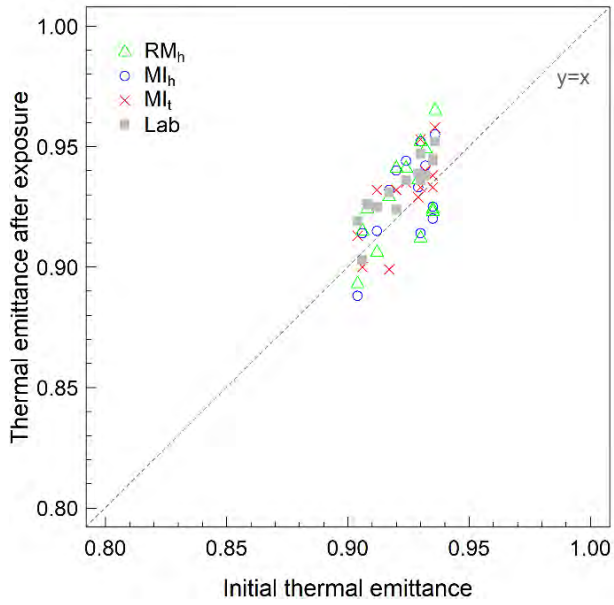

Figure 10. Thermal emittance at the end of the natural aging campaign (T48) and laboratory exposure versus the initial thermal emittance of the roofing membranes.

4. Conclusions

Aging can significantly affect the optical-radiative performance of building envelope materials, and thus the durability of whole building components. Cool materials, in particular, can be subject to major albedo losses due to aging, also reducing the achievable cooling energy savings and mitigation potential.

Here, we presented a variant of the laboratory weathering and soiling protocol detailed in ASTM D7897-18, to reproduce the aging conditions in European urban areas, for roofing membranes, clay tiles, and wall finish coats. The spectral and solar reflectance of samples exposed in the laboratory was compared with the minimum two-site average (i.e., average of the minima in Rome and Milan) measured during the natural aging campaign.

The laboratory protocol is repeatable and reproducible with a smaller standard deviation than outdoor aging. We have shown that the protocol can mimic the effect of outdoor exposure on the optical-radiative properties of materials having diverse and complex spectral features, and different surface finishing (from smooth to rough) and applications, namely both walls and roofing. Moreover, it can be tuned and expanded to other contexts regulating the spraying time and varying the number of weathering cycles, without major changes of the soiling mix. We argue this considering the perfect match between the results from laboratory and natural exposure for different materials having complex spectral features. The most challenging features to be reproduced are the effect of different smoothness and physical degradation, even if the latter does not jeopardize the use of the material.

The need to tune the protocol is not limited to the application in a different context (e.g., another country), but also in the same context years after the initial tuning, as environmental air quality changes with time as a result of technology evolution, emission control policies, and their implementation. Then, the portability of the protocol might be limited to the context where the sources of black carbon and other contaminants are similar, like major urban areas.

The protocol here presented is not an accelerated aging procedure and thus cannot reproduce the reflectance loss of materials subject to major physical degradation, which would

require a significantly increased number of weathering cycles. We demonstrated that soiling is not a “cosmetic” effect of the deposition of contaminants, but it is interrelated to chemical and physical changes in the material. Instead, this protocol has to be used as an essential phase to be incorporated in durability or service life prediction laboratory procedures. Biological growth cannot be reproduced by this protocol, and a dedicated phase is the subject of further research and under development.

We have shown that to improve the laboratory exposure protocols further, the procedures to conduct natural aging campaigns need refinement. Finally, the results of laboratory exposures should be compared to those of multiple exposure campaigns (e.g., three) started at subsequent years, lasting more than three years, and including a set of benchmark materials offering a diverse set of responses to weathering and soiling.

Acknowledgments

This work was supported by the Italian Ministry for Economic Development with the project "Invecchiamento e sporcamento di cool materials: esposizione naturale e accelerata"; by Politecnico di Milano & Agenzia delle Entrate (Italian Revenue Agency) with the project "Cinque per mille junior - Rivestimenti fluorurati avanzati per superfici edilizie ad alte prestazioni"; and by the Assistant Secretary for Energy Efficiency and Renewable Energy, Building Technologies Office of the US Department of Energy under Contract No. DE-AC02-05CH11231. We also recognize the significant support from several industrial collaborators, who provided the roofing and wall samples for natural exposure and laboratory testing. We thank the staff of Osservatorio Meteo Milano Duomo for the validation of weather data of the station at Politecnico di Milano.

References

[1] H. Akbari, C. Cartalis, D. Kolokotsa, A. Muscio, A.L. Pisello, F. Rossi, M. Santamouris, A. Synnefa, N.H. Wong, M. Zinzi, Local climate change and urban heat island mitigation techniques – the state of the art, J. Civ. Eng. Manag. 22 (2016) 1–16. https://doi.org/10.3846/13923730.2015.1111934.

[2] H. Akbari, S. Menon, A. Rosenfeld, Global cooling: increasing world-wide urban albedos to offset CO2, Clim. Change. 94 (2008) 275–286. https://doi.org/10.1007/s10584-008-9515-9.

[3] M. Santamouris, Cooling the cities – A review of reflective and green roof mitigation technologies to fight heat island and improve comfort in urban environments, Sol. Energy. 103 (2014) 682–703. https://doi.org/10.1016/j.solener.2012.07.003.

[4] M. Santamouris, Cooling the buildings – past, present and future, Energy Build. 128 (2016) 617–638. https://doi.org/10.1016/j.enbuild.2016.07.034.

[5] P.J. Rosado, R. Levinson, Potential benefits of cool walls on residential and commercial buildings across California and the United States: Conserving energy, saving money, and reducing emission of greenhouse gases and air pollutants, Energy Build. (2019). https://doi.org/10.1016/J.ENBUILD.2019.02.028.

[6] J. Zhang, A. Mohegh, Y. Li, R. Levinson, G. Ban-Weiss, Systematic Comparison of the Influence of Cool Wall versus Cool Roof Adoption on Urban Climate in the Los Angeles Basin, Environ. Sci. Technol. 52 (2018) 11188–11197. https://doi.org/10.1021/acs.est.8b00732.

[7] R. Paolini, A. Zani, T. Poli, F. Antretter, M. Zinzi, Natural aging of cool walls: Impact on solar reflectance, sensitivity to thermal shocks and building energy needs, Energy Build. 153 (2017) 287–296. https://doi.org/10.1016/j.enbuild.2017.08.017.

[8] European Commission, Guidance Paper F - Durability and the Construction Products Directive, 2004. https://eurocodes.jrc.ec.europa.eu/doc/gpf.pdf (accessed July 29, 2019).

[9] ISO, ISO 6707-1:2017 - Buildings and civil engineering works - Vocabulary - Part 1: General terms, (2017). https://www.iso.org/standard/72244.html (accessed July 29, 2019).

[10] P. Berdahl, H. Akbari, R. Levinson, W.A. Miller, Weathering of roofing materials – An overview, Constr. Build. Mater. 22 (2008) 423–433. https://doi.org/10.1016/j.conbuildmat.2006.10.015.

[11] M.D. Cheng, S.M. Pfiffner, W.A. Miller, P. Berdahl, Chemical and microbial effects of atmospheric particles on the performance of steep-slope roofing materials, Build. Environ. 46 (2011) 999–1010. https://doi.org/10.1016/j.buildenv.2010.10.025.

[12] R. Paolini, M. Zinzi, T. Poli, E. Carnielo, A.G. Mainini, Effect of ageing on solar spectral reflectance of roofing membranes: natural exposure in Roma and Milano and the impact on the energy needs of commercial buildings, Energy Build. 84 (2014) 333–343. https://doi.org/10.1016/j.enbuild.2014.08.008.

[13] M. Sleiman, G. Ban-Weiss, H.E. Gilbert, D. François, P. Berdahl, T.W. Kirchstetter, H. Destaillats, R. Levinson, Soiling of building envelope surfaces and its effect on solar reflectance—Part I: Analysis of roofing product databases, Sol. Energy Mater. Sol. Cells. 95 (2011) 3385–3399. https://doi.org/10.1016/j.solmat.2011.08.002.

[14] M. Sleiman, T.W. Kirchstetter, P. Berdahl, H.E. Gilbert, S. Quelen, L. Marlot, C. V. Preble, S. Chen, A. Montalbano, O. Rosseler, H. Akbari, R. Levinson, H. Destaillats, Soiling of building envelope surfaces and its effect on solar reflectance – Part II: Development of an accelerated aging method for roofing materials, Sol. Energy Mater. Sol. Cells. 122 (2014) 271–281. https://doi.org/10.1016/j.solmat.2013.11.028.

[15] O. Favez, H. Cachier, a Chabas, P. Ausset, R. Lefevre, Crossed optical and chemical evaluations of modern glass soiling in various European urban environments, Atmos. Environ. 40 (2006) 7192–7204. https://doi.org/10.1016/j.atmosenv.2006.06.022.

[16] K. Dornelles, R. Caram, E. Sichieri, Natural Weathering of Cool Coatings and its Effect on Solar Reflectance of Roof Surfaces, Energy Procedia. 78 (2015) 1587–1592. https://doi.org/10.1016/j.egypro.2015.11.216.

[17] N.L. Alchapar, E.N. Correa, Aging of roof coatings. Solar reflectance stability according to their morphological characteristics, Constr. Build. Mater. 102 (2016) 297–305. https://doi.org/10.1016/j.conbuildmat.2015.11.005.

[18] H. Takebayashi, K. Miki, K. Sakai, Y. Murata, T. Matsumoto, S. Wada, T. Aoyama, Experimental examination of solar reflectance of high-reflectance paint in Japan with natural and accelerated aging, Energy Build. 114 (2016) 173–179. https://doi.org/10.1016/J.ENBUILD.2015.06.019.

[19] T. Aoyama, T. Sonoda, Y. Nakanishi, J. Tanabe, H. Takebayashi, Study on aging of solar reflectance of the self-cleaning high reflectance coating, Energy Build. 157 (2017) 92–100. https://doi.org/10.1016/J.ENBUILD.2017.02.021.

[20] S.S. Chen, H. Destaillats, J. Ge, R.M. Levinson, Calibration of laboratory aging practice to replicate changes to roof albedo in a Chinese city, E-Scholarship Repository, Berkeley, CA (United States), 2018. https://doi.org/10.2172/1460338.

[21] D. Shi, C. Zhuang, C. Lin, X. Zhao, D. Chen, Y. Gao, R. Levinson, Effects of natural soiling and weathering on cool roof energy savings for dormitory buildings in Chinese cities with hot summers, Sol. Energy Mater. Sol. Cells. 200 (2019) 110016. https://doi.org/10.1016/J.SOLMAT.2019.110016.

[22] T.W. Kirchstetter, T. Novakov, P. V. Hobbs, Evidence that the spectral dependence of light absorption by aerosols is affected by organic carbon, J. Geophys. Res. Atmos. 109 (2004) n/a-n/a. https://doi.org/10.1029/2004JD004999.

[23] P. Krishnan, M.H. Zhang, L.E. Yu, Removal of black carbon using photocatalytic silicate-based coating: Laboratory and field studies, J. Clean. Prod. 183 (2018) 436–448. https://doi.org/10.1016/J.JCLEPRO.2018.02.149.

[24] M. Lettieri, D. Colangiuli, M. Masieri, A. Calia, Field performances of nanosized TiO2 coated limestone for a self-cleaning building surface in an urban environment, Build. Environ. (2018). https://doi.org/10.1016/J.BUILDENV.2018.10.037.

[25] R. Paolini, M. Sleiman, M.P. Pedeferri, M.V. Diamanti, TiO2 alterations with natural aging: Unveiling the role of nitric acid on NIR reflectance, Sol. Energy Mater. Sol. Cells. 157 (2016) 791–797. https://doi.org/10.1016/j.solmat.2016.07.052.

[26] X. Tang, L. Ughetta, S.K. Shannon, S. Houzé de l'Aulnoit, S. Chen, R.A.T. Gould, M.L. Russell, J. Zhang, G. Ban-Weiss, R.L.A. Everman, F.W. Klink, R. Levinson, H. Destaillats, De-pollution efficacy of photocatalytic roofing granules, Build. Environ. 160 (2019) 106058. https://doi.org/10.1016/J.BUILDENV.2019.03.056.

[27] A. Maury-Ramirez, K. Demeestere, N. De Belie, Photocatalytic activity of titanium dioxide nanoparticle coatings applied on autoclaved aerated concrete: effect of weathering on coating physical characteristics and gaseous toluene removal., J. Hazard. Mater. 211–212 (2012) 218–25. https://doi.org/10.1016/j.jhazmat.2011.12.037.

[28] M.V. Diamanti, R. Paolini, M. Rossini, A.B. Aslan, M. Zinzi, T. Poli, M.P. Pedeferri, Long term self-cleaning and photocatalytic performance of anatase added mortars exposed to the urban environment, Constr. Build. Mater. 96 (2015) 270–278. https://doi.org/10.1016/j.conbuildmat.2015.08.028.

[29] E. Mastrapostoli, M. Santamouris, D. Kolokotsa, P. Vassilis, D. Venieri, K. Gompakis, On the aging of cool roofs. Measure of the optical degradation, chemical and biological analysis and assessment of the energy impact, Energy Build. 114 (2015) 191–199. https://doi.org/10.1016/j.enbuild.2015.05.030.

[30] M.D. Cheng, S.L. Allman, D.E. Graham, K.R. Cheng, S.M. Pfiffner, T.A. Vishnivetskaya, A.O. Desjarlais, Surface reflectance degradation by microbial communities, J. Build. Phys. 40 (2016) 263–277. https://doi.org/10.1177/1744259115611866.

[31] C. Ferrari, G. Santunione, A. Libbra, A. Muscio, E. Sgarbi, C. Siligardi, G.S. Barozzi, Review On The Influence Of Biological Deterioration On The Surface Properties Of Building Materials: Organisms, Materials, And Methods, Int. J. Des. Nat. Ecodynamics. 10 (2015) 21–39. https://doi.org/10.2495/DNE-V10-N1-21-39.

[32] G. Santunione, C. Ferrari, C. Siligardi, A. Muscio, E. Sgarbi, Accelerated biological ageing of solar reflective and aesthetically relevant building materials, Adv. Build. Energy Res. (2018) 1–18. https://doi.org/10.1080/17512549.2018.1488616.

[33] E. Di Giuseppe, Nearly Zero Energy Buildings and Proliferation of Microorganisms, Springer International Publishing, Cham, 2013. https://doi.org/10.1007/978-3-319-02356-4.

[34] Cool Roof Rating Council, CRRC rated products directory, (2018). http://coolroofs.org/products/results (accessed February 9, 2018).

[35] ASTM International, ASTM D 7897-18. Standard Practice for Laboratory Soiling and Weathering of Roofing Materials to Simulate Effects of Natural Exposure on Solar Reflectance and Thermal Emittance, (2018). https://doi.org/10.1520/D7897-18.

[36] EOTA, ETAG004 - External Thermal Insulation Composite Systems with Rendering, (2013). https://www.eota.eu/en-GB/content/etags/26/ (accessed July 29, 2019).

[37] ASTM International, ASTM E2110 - 17 Standard Terminology for Exterior Insulation and Finish Systems (EIFS), (2017). https://doi.org/10.1520/E2110-17.

[38] ASTM International, ASTM G 7-05. Standard Practice for Atmospheric Environmental Exposure Testing of Nonmetallic Materials, (2005).

[39] ISO, ISO 2810. Paints and varnishes – Natural weathering of coatings - Exposure and assessment, (2004).

[40] ASTM International, ASTM E 903-12. Standard Test Method for Solar Absorptance, Reflectance, and Transmittance of Materials Using Integrating Spheres, (2012). https://doi.org/10.1520/E0903-12.

[41] R. Levinson, H. Akbari, P. Berdahl, Measuring solar reflectance-Part I: Defining a metric that accurately predicts solar heat gain, Sol. Energy. 84 (2010) 1717–1744. https://doi.org/10.1016/j.solener.2010.04.018.

[42] A. Synnefa, A. Pantazaras, M. Santamouris, E.M.D. Bozonnet, M. Doya, M. Zinzi, A. Muscio, A. Libbra, C. Ferrari, V. Coccia, F. Rossi, D. Kolokotsa, Interlaboratory Comparison of Cool Roofing Material Measurement Methods, in: 34th AIVC Conf., Athens, Greece, 2013.

[43] CEN, EN 15976. Flexible sheets for waterproofing. Determination of emissivity, (2011).

[44] M. Rubin, J. Johnson, NFRC Interlaboratory Comparison on Optical Properties, Berkeley, CA, USA, 2007. http://gaia.lbl.gov/btech/papers/501.pdf.

[45] ASTM International, ASTM C1371-15. Standard Test Method for Determination of Emittance of Materials Near Room Temperature Using Portable Emissometers, (2015). https://doi.org/10.1520/C1371-15.

[46] SIA, SIA 271. Waterproofing for buildings, (2007).

[47] IGLAE, Codice di pratica delle impermeabilizzazioni (Practice code for waterproofing. In Italian), 2012. http://www.iglae.org.

[48] JSTM, JSTM J7601. Test Method of Outdoor Exposure for Dirt Collection on Exterior Building Wall Materials and Finishes, (2003).

[49] Y. Kitsutaka, Accelerated Soiling Test Method for Painted Materials, in: Int. Work. Adv. Cool Roof Res. Protoc. Stand. Policies Accel. Aging, Berkeley Marina, Berkeley, CA, USA, 2011. https://sites.google.com/a/lbl.gov/coolroofs2011/.

[50] R. Paolini, A. Zani, M. MeshkinKiya, V.L.V.L. Castaldo, A.L.A.L. Pisello, F. Antretter, T. Poli, F. Cotana, The hygrothermal performance of residential buildings at urban and rural sites: Sensible and latent energy loads and indoor environmental conditions, Energy Build. 152 (2017) 792–803. https://doi.org/10.1016/j.enbuild.2016.11.018.

[51] M. Zinzi, E. Carnielo, B. Mattoni, On the relation between urban climate and energy performance of buildings. A three-years experience in Rome, Italy, Appl. Energy. 221 (2018) 148–160. https://doi.org/10.1016/J.APENERGY.2018.03.192.

[52] S. Curci, C. Lavecchia, G. Frustaci, R. Paolini, S. Pilati, C. Paganelli, Assessing measurement uncertainty in meteorology in urban environments, Meas. Sci. Technol. 28 (2017). https://doi.org/10.1088/1361-6501/aa7ec1.

[53] ARPA Lombardia, Air quality data of ARPA Lombardia, Agenzia Regionale per la Protezione Ambientale della Lombardia (Environmental Protection Agency of Lombardia region, Italy), (2015). http://www2.arpalombardia.it/.

[54] ARPA Lazio, Air quality data of ARPA Lazio, Agenzia Regionale per la Protezione Ambientale del Lazio (Environmental Protection Agency of Lazio region, Italy), (2015). www.arpalazio.it.

[55] ARSIAL, Servizio Integrato Agrometeorologico Regione Lazio. Weather station RM26CME - via Lanciani, Roma, Italy, (n.d.). http://www.arsial.it/portalearsial/agrometeo/C2.asp (accessed June 28, 2019).

[56] N. Moise, M. Rogers, J. Rush, P. Shah, Annual Air Quality Monitoring Report 2010, Cleveland, OH, USA, 2010. http://www.clevelandhealth.org/assets/documents/health/communicable_disease/air_quality_report_2010_final_draft.pdf.

[57] Cool Roofing Rating Council, ANSI/CRRC S100-2016. Standard Test Methods for Determining Radiative Properties of Materials, (2018). https://coolroofs.org/documents/ANSI-CRRC_S100-2016_Final.pdf (accessed August 15, 2019).

[58] EOTA, Assessment of working life of Products. Guidance document 003, (1999). http://www.eota.eu/handlers/download.ashx?filename=guidance-documents%2Fgd003.pdf.

[59] M. Sleiman, S. Chen, H.E. Gilbert, T.W. Kirchstetter, P. Berdahl, E. Bibian, L.S. Bruckman, D. Cremona, R.H. French, D.A. Gordon, M. Emiliani, J. Kable, L. Ma, M. Martarelli, R. Paolini, M. Prestia, J. Renowden, G.M. Revel, O. Rosseler, M. Shiao, G. Terraneo, T. Yang, L. Yu, M. Zinzi, H. Akbari, R. Levinson, H. Destaillats, Soiling of building envelope surfaces and its effect on solar reflectance – Part III: Interlaboratory study of an accelerated aging method for roofing materials, Sol. Energy Mater. Sol. Cells. 143 (2015) 581–590. https://doi.org/10.1016/j.solmat.2015.07.031.

[60] ASTM International, ASTM G154 - 12a Standard Practice for Operating Fluorescent Ultraviolet (UV) Lamp Apparatus for Exposure of Nonmetallic Materials, (2012). https://doi.org/10.1520/G0154-12.

Supplementary Material

Table S1. Climate and air quality features in Rome and Milan. Air quality data from ARPA Lazio [54] and ARPA Lombardia [53] (regional environmental protection agencies). Data correspond to the period of natural exposure (April 2012 – April 2016). The air quality stations in Rome are Cipro station (41.9064° N, 12.4476° E), and Villa Ada (41.9329° N, Long: 12.5070° E). The air quality station in Milan is Citta' Studi via Pascal (45.4784° N, 9.2311° E).

Quantity	**Rome**			**Milan**		
	98th percentile	Median	2nd percentile	98th percentile	Median	2nd percentile
NO_x total (µg m^{-3})	281	51	11	500	53	11
NO_2 (µg m^{-3})	90	37	9	105	39	8
SO_2 (µg m^{-3})	5	0	0	11	4	0
$PM_{2.5}$ (µg m^{-3})	43	14	5	87	23	4
PM_{10} (µg m^{-3})	60	23	9	105	32	8

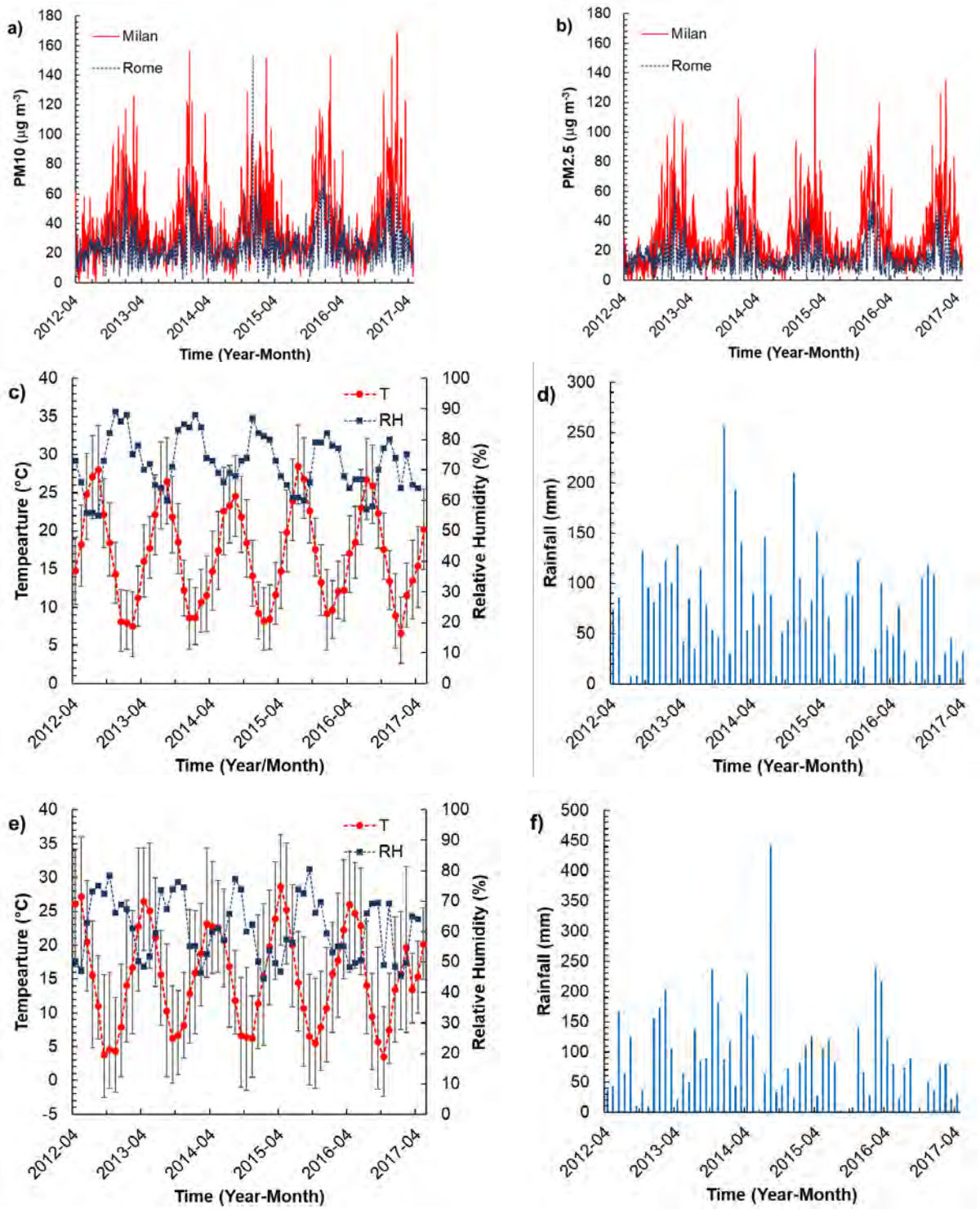

Figure S1. Air quality and climate at the exposure sites starting from April 2012. (a) PM10 and (b) PM2.5 average daily concentrations in Rome and Milan. (c) Monthly averages of air temperature and relative humidity and (d) monthly rainfall in Rome. Data from the weather station in via Lanciani of Servizio Integrato Agrometeorologico Regione Lazio [55], (e) Monthly averages of air temperature and relative humidity and (f) monthly rainfall in Milano, from a weather station at the exposure site [52]. The whiskers indicate the maximum and minimum monthly records.

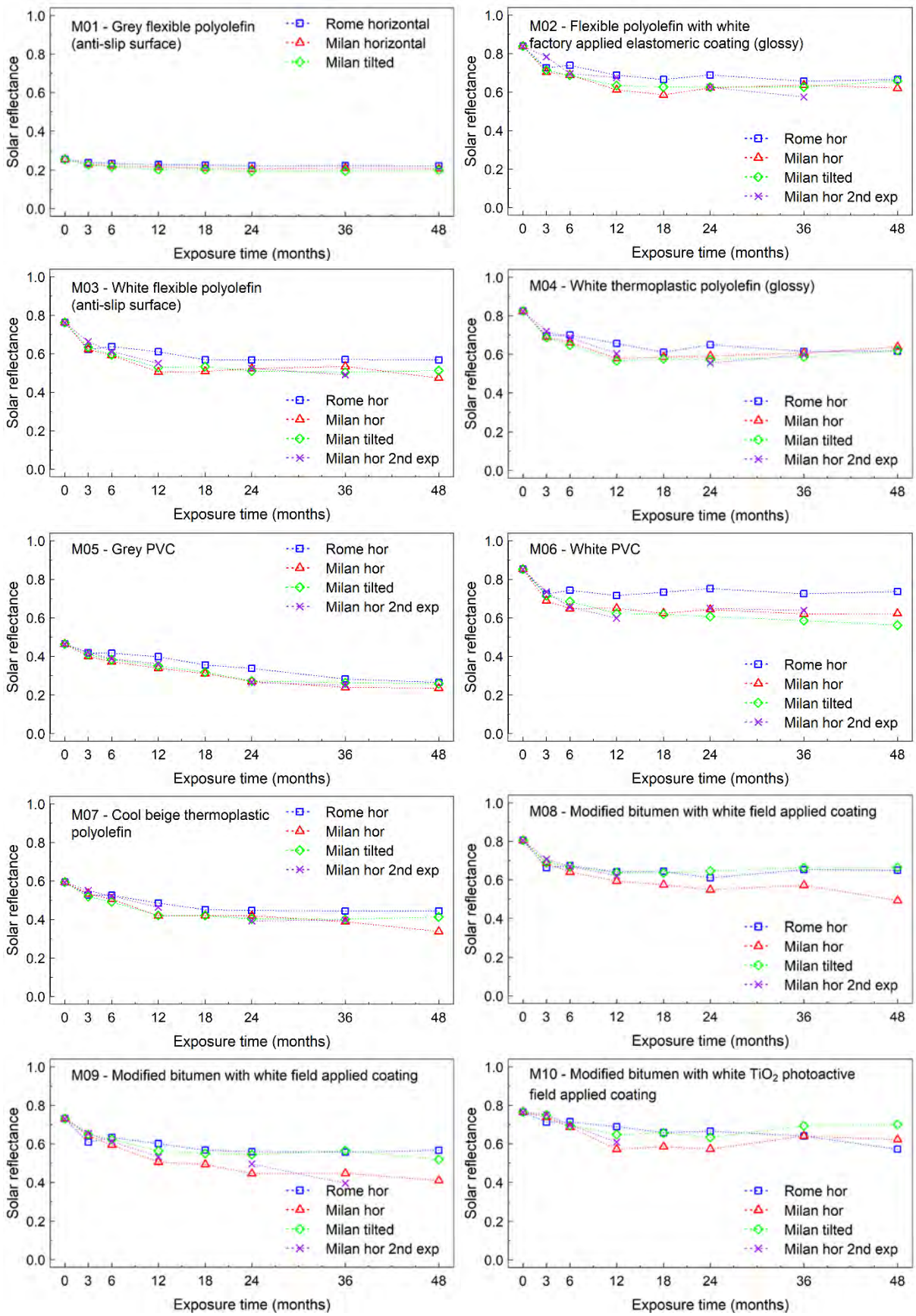

Figure S2. Reflectance vs. exposure time for membranes 1-10.

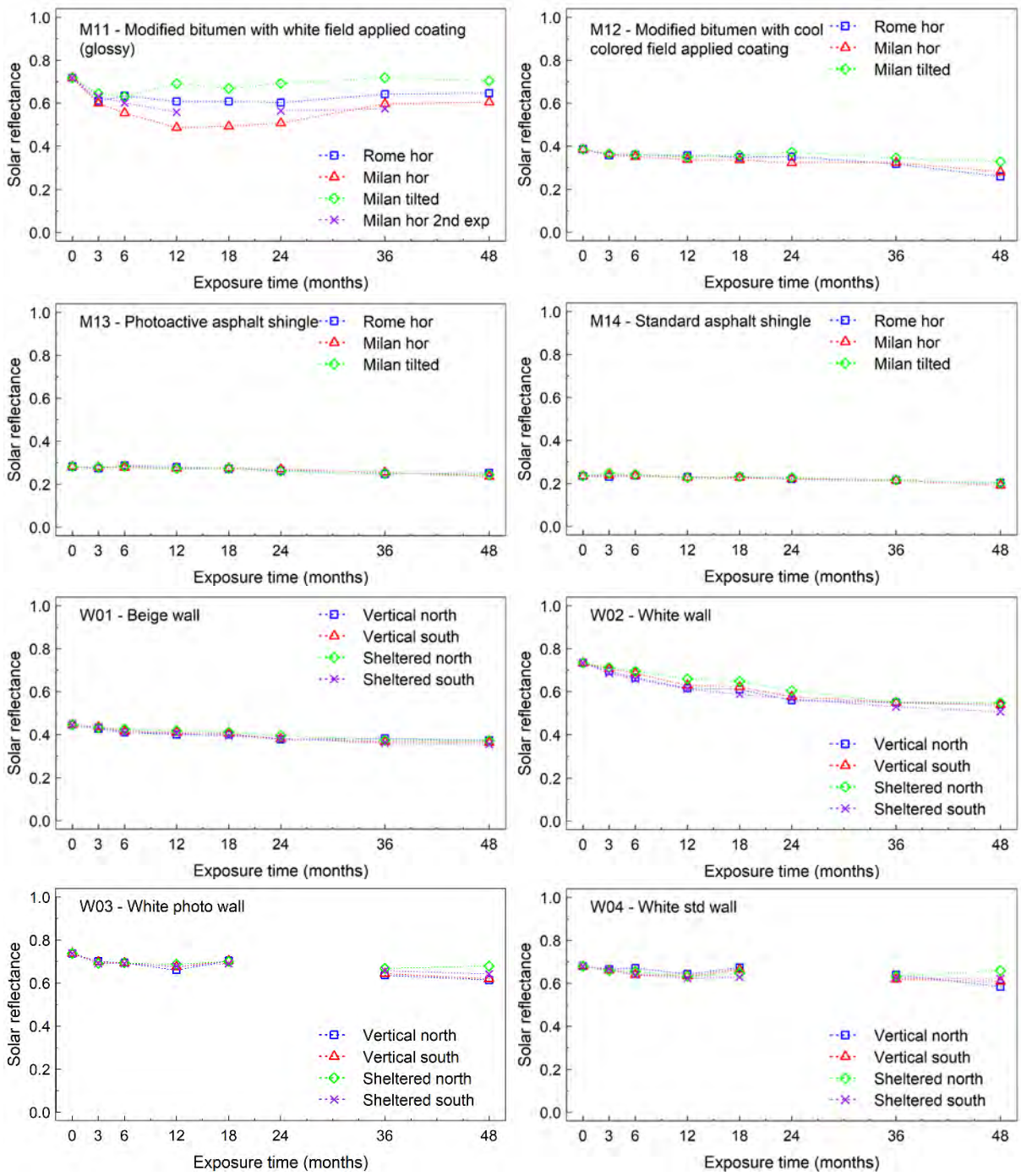

Figure S3. Reflectance vs. exposure time for membranes 11-14 and wall materials 1 - 4.

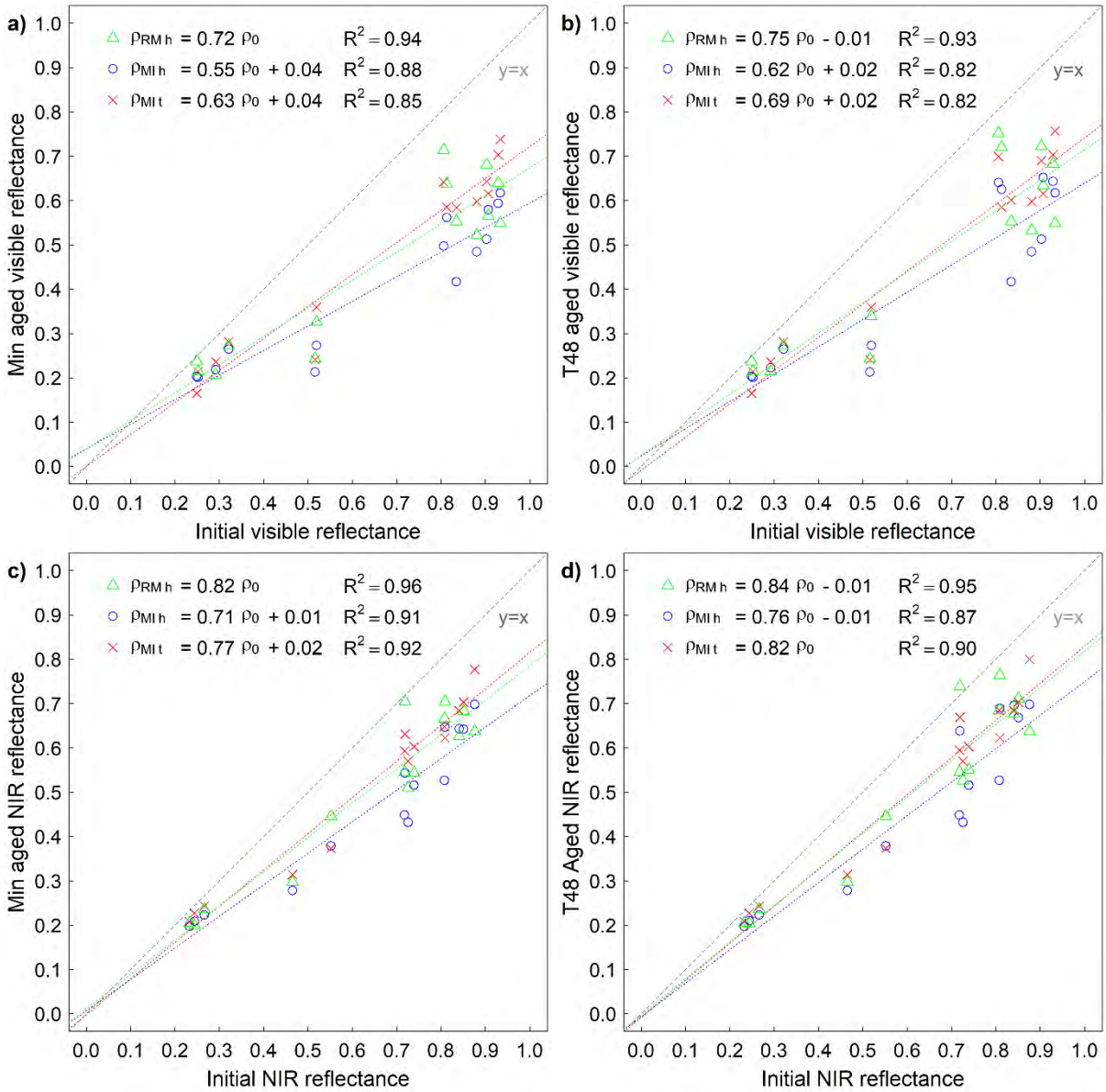

Figure S4. Regressions to initial value of (a) minimum visible reflectance measured in the first 48 months, (b) visible reflectance measured at 48 months, (c) minimum near infrared reflectance measured in the first 48 months, and (d) near infrared reflectance measured at 48 months , shown for horizontal exposure in Rome and Milan and tilted exposure in Milan.

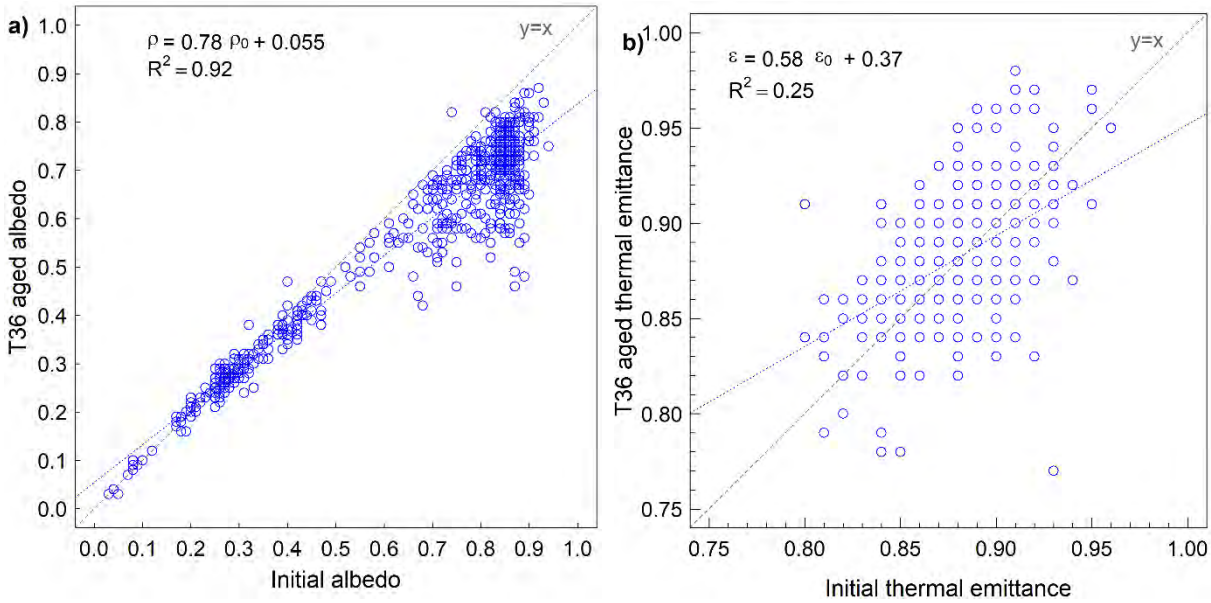

Figure S5. Three-years aged vs. initial (a) albedo and (b) thermal emittance. Elaboration on CRRC three-site average data [34] for asphalt shingles, modified bitumen, coatings, single-ply membranes, and tiles.

Metadata and Dataset Description

© 2019. This dataset is made available under the CC-BY-NC-ND 4.0 license

http://creativecommons.org/licenses/by-nc-nd/4.0/

Disclaimer

The dataset was prepared as an account of work sponsored by the Italian Revenue Agency and the Italian Ministry of Economic Development, with the initial stages of the laboratory exposure adaptation supported also by the United States Department of Energy. Part of the data analysis was conducted while at the University of New South Wales, Australia, with Riccardo Paolini's position sponsored by the fund Anita Lawrence Chair in High Performance Architecture at the Faculty of Built Environment. While this document is believed to contain correct information, neither the Italian Government, the United States Government, nor any agency thereof, nor the Research Institutions to which the authors are affiliated, nor any of their employees, make any warranty, express or implied, or assumes any legal responsibility for the accuracy, completeness, or usefulness of any information, apparatus, product, or process disclosed, or represents that its use would not infringe privately owned rights. Reference herein to any specific commercial product process, or service by its trade name, trademark, manufacturer, or otherwise, does not necessarily constitute or imply its endorsement, recommendation, or favouring by the Italian or the United States Government or any agency thereof, or the Research Institutions to which the authors are affiliated. Further, the dataset does not make any reference to commercial products and commercial technologies and the data cannot be used neither to promote nor denigrate any product or company.

Use of the dataset

For any question concerning the dataset or supplementary information, please contact Riccardo Paolini

r.paolini@unsw.edu.au, RPaolini@LBL.gov, riccardo.paolini@polimi.it

The publication of work substantially relying on the dataset shall be discussed with the Authors, who retain the intellectual property of the data. Derivative work shall acknowledge the dataset and city the study that produced it.

Composition of the dataset

Solar spectral irradiance used to compute broadband reflectance values

File: Sol_Spec_Irr_2015-06-30.txt

Spectral irradiance distribution used: AM1GH as in Levinson et al. (2010). Computed by Ronnen with SMARTS 2.9.5 https://solarconsultingservices.com/smarts.php

Also included
ISO 9050: 2003. (AM1.5GH). From the standard. The poor spectral resolution in the near infrared (@50 nm) is from the standard.

AM1.5GH37deg to comply with ASTM E 1980 for Solar Reflectance Index calculation (computed by Riccardo with SMARTS 2.9.5)

Note: ASTM E1980 wants the solar reflectance to be computed with the spectrum of ASTM G 173 Tables for Reference Solar Spectral Irradiances: Direct Normal and Hemispherical on 37° Tilted Surface.

Natural exposure data

Unaged reflectance values (3 scans per material)
File: T0_all-meas_2014-03-24.txt

Rome natural exposure data – Exposure campaign started in April 2012
Rome, 3 months results. File: T3_RO_2013-05-15.txt
Rome, 6 months results. File: T6_RO_2013-05-15.txt
Rome, 12 months results. File: T12_RO_2013-05-15.txt
Rome, 18 months results. File: T18_RO_2013-11-04.txt
Rome, 24 months results. File: T24_RO_2014-07-31.txt
Rome, 36 months results. File: T36_RO_2015-06-05.txt
Rome, 48 months results. File: T48_RO_2016-10-20.txt

Milan natural exposure data – Exposure campaign started in April 2012
Milan, 3 months results. File: T3_MI_2013-02-03.txt
Milan, 6 months results. File: T6_MI_2013-02-03.txt
Milan, 12 months results. File: T12_MI_2013-05-21.txt
Milan, 18 months results. File: T18_MI_2014-03-22.txt
Milan, 24 months results. File: T24_MI_2014-07-24.txt
Milan, 36 months results. File: T36_MI_2015-06-05.txt
Milan, 48 months results. File: T48_MI_2016-10-21.txt

Milan natural exposure data – Second exposure campaign started in April 2013
Milan II, 3 months results. File: T3-2013_MI-hor.txt
Milan II, 3 months results. File: T6-2013_MI-hor.txt
Milan II, 3 months results. File: T12-2013_MI-hor.txt

Milan II, 3 months results. File: T24-2013_MI-hor.txt
Milan II, 3 months results. File: T36-2013_MI-hor.txt

Measurements of three spots per specimen at the end of the exposure (2012 campaign)
Milan, 3 spots, 48 months results. File: T48_MI_3spots.txt
Rome, 3 spots, 48 months results. File: ROMA_T48_3spots.txt

Measurements of tiles fragments from big tiles at the end of the 2012 exposure campaign
Milan and Rome, 60 months results tiles only (average value). File: T60_Tiles_Rome&Milan_AVG.txt

Laboratory exposure

Unexposed reflectance values
File: Acc_T0_2017-04-13.txt
Note: time zero measurements were performed on the samples to be aged in the lab (necessary as some age also in the drawer; aging the original set wasn't possible for all materials)

Laboratory exposed reflectance values
File: Acc_Tf_2017-04-13.txt

Naming and conventions used in the files
Aging time = T0, T3, ..., T48 (the number is the duration of the exposure in months)
For lab exposure there is only T0 and Tf (i.e., final)

Specimen name
Each specimen has a six digits code. This system was developed when the software of the spectrometer allowed only for six digits in the sample name.

1st digit is the location: 1 = Rome; 2 = Milan; 6 = Milan second campaign (started in 2013); L = Lab (adapted version of ASTM D7895-18, as detailed in the paper).
2nd & 3rd digits are the material code: 01-17 = membrane; 31-43 = facade; ...

4th digit is orientation: 1 = north, 2 = south (south is set by default also for horizontal / low sloped exposure)

5th digit is the slope: 1 = low sloped (~2% slope); 2 = 30 % slope (for roof tiles); 3 = 45 deg slope; 4 = vertical; 5 = vertical sheltered

6th digit is the sample replicate (from 1 to 3)

scan number
.n (n = 1-3), after the sample name (if more than one scan was performed per sample)

Example

T0_L0121.1

T0	Time zero measurement
L	lab exposure
01	roofing membrane 01
2	south
1	low sloped exposure
1	sample 1
1	scan 1 (of 3)

south and low sloped exposure digits are retained to indicate of what natural aging condition the lab exposure is representative

The correspondence between specimen code used in the scans and name used in the paper is given in Tables 1 and 2.

Correspondence between products and codes in the files

Table 1. Selected building envelope products and initial solar reflectance and thermal emittance.

Code	**Description**	Rome hor (2012)	Milan hor (2012)	Milan 45° (2012)	Milan hor (2013)	Lab
M01	Grey flexible polyolefin (matte and with anti-slip surface)	10121-1/2/3	20121-1/2/3	20123-1/2/3	N/A	L01
M02	Grey flexible polyolefin with white factory-applied elastomeric coating (glossy)	10221-1/2/3	20221-1/2/3	20221-1/2/3	60221-1/2/3	L01
M03	White flexible polyolefin (matte and with anti-slip surface)	10321-1/2/3	20321-1/2/3	20321-1/2/3	60321-1/2/3	L01
M04	White thermoplastic polyolefin (glossy)	10421-1/2/3	20421-1/2/3	20421-1/2/3	60421-1/2/3	L01
M05	Grey PVC membrane.	10521-1/2/3	20521-1/2/3	20521-1/2/3	60621-1/2/3	L01
M06	White PVC membrane (matte)	10621-1/2/3	20621-1/2/3	20621-1/2/3	60621-1/2/3	L01
M07	Cool beige thermoplastic polyolefin (matte)	10721-1/2/3	20721-1/2/3	20721-1/2/3	60721-1/2/3	L01
M08	Modified-bitumen with extra white field-applied coating	10821-1/2/3	20821-1/2/3	20821-1/2/3	60821-1/2/3	L01
M09	Modified-bitumen with white field-applied coating	10921-1/2/3	20921-1/2/3	20921-1/2/3	60921-1/2/3	L01
M10	Modified-bitumen with white TiO_2 photoactive field applied coating	181121-1/2/3	281121-1/2/3	281123-1/2/3	681121-1/2/3	L10
M11	Modified-bitumen with white field-applied coating type B (glossy)	182121-1/2/3	282121-1/2/3	282123-1/2/3	682121-1/2/3	L11
M12	Modified-bitumen with cool colored field-applied coating	182121-1/2/3	282121-1/2/3	282123-1/2/3	682121-1/2/3	L12
M13	Photoactive asphalt roll (modified-bitumen with granules)	183121-1/2/3	283121-1/2/3	283123-1/2/3	N/A	L13
M14	Standard asphalt roll (modified-bitumen with granules)	184121-1/2/3	284121-1/2/3	284 123-1/2/3	N/A	L14

Table 2. Selected building envelope products and initial solar reflectance and thermal emittance.

Code	**Description**	Rome north (2012)	Rome south (2012)	Milan north (2012)	Milan south (2012)	Milan north sheltered (2012)	Milan south sheltered (2012)	Lab
T01	Red clay tile	11011-1-2-3	11022-1-2-3	21012-1-2-3	21022-1-2-3	N/A	N/A	LTr
T02	White paint on clay tile	11111-1-2-3	11122-1-2-3	21112-1-2-3	21122-1-2-3	N/A	N/A	LTw
W01	Beige wall finish coat (rough)	N/A	N/A	23014-1/2/3	23024-1/2/3	23015-1/2/3	23025-1/2/3	LW01
W02	White wall finish coat (rough)	N/A	N/A	23114-1/2/3	23124-1/2/3	23115-1/2/3	23125-1/2/3	LW02
W03	White fiber reinforced mortar (photoactive)	N/A	N/A	23414-1/2/3	23424-1/2/3	23415-1/2/3	23425-1/2/3	LW03
W04	White fiber reinforced mortar (standard)	N/A	N/A	23314-1/2/3	23324-1/2/3	23315-1/2/3	23325-1/2/3	LW04